1-1-2017

Dynamic Analysis for Characterization of Novel Biomass Based Composities

Aarsh Jigish Shah
University of Mississippi

DYNAMIC ANALYSIS FOR CHARACTERIZATION OF NOVEL BIOMASS BASED COMPOSITIES

A Thesis

presented in partial fulfillment of requirements

for the degree of Master of Science

in the Department of Mechanical Engineering

The University of Mississippi

by

AARSH SHAH

December 2017

ABSTRACT

Resources from forests constitute a significant asset of Mississippi State. Forests cover around 19.7 million acres (65%) of the total land area of Mississippi. Total annual economic impact of Mississippi's forest products is about $17 billion. Creation of high-value products will lead to a number of economic benefits to the region. This work focuses on the study of bio-composite. Bio-composite materials are a 'Green' alternative to conventional materials which are readily recyclable and biodegradable. Taylor made properties are achievable in bio-composites, this being one of the significant advantages.

Producing biodegradable products has become a necessity due to petroleum-based products being a finite resource and having more potential to harm the environment.

In this work, a number of bio-composites were characterized by their mechanical properties. High strain rate behavior under three different strain rates, influence of damage in the natural frequency of the bio-composites, comparison between dynamic modulus of elasticity under flexural vibration and Young's modulus, variation in Poisson's ratio were studied.

ACKNOWLEDGMENTS

I would like to first thank my advisor, Dr. Tejas S Pandya, for his constant support and assistance throughout my research and my journey at The University of Mississippi.

I would also like to thank my Thesis Committee, Dr. P. Raju Mantena, Dr. Jeffrey Roux for their guidance in preparing my thesis. I would also like to express my most profound gratitude to the Department Chair, Dr. A. M. Rajendran for guiding and supporting me throughout this journey

I would also like to thank the staff and faculty members in the Department of Mechanical Engineering for their contributions during my graduate study. I would like convey my special thanks to Dr. P. Raju Mantena, Dr. Street, Damian, and Matt Lowe, for helping out and providing assistance with many aspects of my research and my colleagues Maharshi, Suman, and other department colleagues.

Lastly, I would like to thank my parents, my brother for their immense support throughout my progress during my Master of Science in Mechanical Engineering.

TABLE OF CONTENTS

LIST OF TABELS

LIST OF FIGURES

CHAPTER I

INTRODUCTION TO BIO-COMPOSITIES

Due to increasing environmental awareness, the development of natural fiber composite materials or environmentally friendly composite has been a great topic of discussion lately. As supplements to polymer-based materials, a type of renewable sources and next generation reinforcement; natural fibers are used. Natural fibers are one such competent material which restores the use of synthetic materials and its related products for less weight and energy conservation applications. The application of natural fiber reinforced polymer composites and natural-based resins for changing present time synthetic polymer or glass fiber bolstered materials is huge in car and aircraft industries. It has been actively growing specific styles of natural fibers, mainly on hemp, flax and sisal and bioresins systems for their indoors components. High specific properties with decrease costs of natural fiber composites are making it appealing for various packages. [1,2]

In recent years, eco-friendly biodegradable polymers and plastics have gained increasing attention because of growing recognition worldwide of the need to reduce global environmental pollution [3-5]. These biodegradable materials can be degraded entirely into natural ecosystems such as active sludge, native soil, lake, and marine. Accordingly, the biodegradability of biodegradable polymers corresponds to the ability to be chemically transformed by the action of biological enzymes or microorganisms [5,6]

Modern society uses Synthetic polymers widely. However, the yearly worldwide disposal of approximately 150 million tons of petrochemical plastics in the commonly used product such as polyolefin in packing, bottle and molding products is a significant environmental problem, especially with the continuously increasing production and consumption of these materials [5,7]. Furthermore, plastic wastes are an undesired pollutant in soil, rivers, and marine enviornments. Because of their resistance to microbial attack, they tend to accumulate in the natural environment.

The U.S. agricultural, forestry, life sciences, and chemical communities have developed a strategic vision [8] for using crops, trees, and agricultural residues to manufacture industrial products, and have identified significant barriers [9] to its implementation. Eco-friendly bio-composites from plant-derived fiber (natural/biofiber) and crop-derived plastics are novel materials of the twenty-first century and would be of great importance to the materials world, only as a solution to growing environmental ultimatum but also as a solution to the uncertainty of petroleum supply [10, 11]. Biopolymers are now moving into conventional use, and the polymers that are biodegradable or on renewable "feedstock" may soon be competing for commodity plastics, as a result of the sales growth of more than 20–30% per year and improvement in the economics of sales [12]. The best examples of biopolymers based on renewable resources are: cellulosic plastics, (PLA), starch plastics, and soy-based plastics, Microbial synthesized biopolymers, i.e., polyhytion droxy alkanoates (PHAs) polymers, have also attracted attention recently. The use of materials from renewable resources is attaining increased importance, and the world's leading industries and manufacturers seek to replace dwindling petrochemical-based feedstock with derived from natural fibers and biopolymers.

1.1 Mechanical properties

Nature of natural fibers such as fiber structure was the primary influence on the Bio-composite reinforced natural fibers, thermal stability, fiber size, fiber loading, distribution, and orientation. Also, processing method and natural fiber surface treatment also affect the bio-composite mechanical properties [13-16]. According to Ahmad et al., mechanical properties are affected by the material's ability to transfer stress exerted from the matrix to fiber particles. Efficiency of stress transfer will determine the high tensile strength [17]

Singh et al. investigate that with the growth of hybrid composites from wood fiber, talc, and a bioplastic, i.e., polyhydroxybutyrate-co-valerate (PHBV) using the extrusion–injection molding, with the further reinforcement of micro-sized talc in it, the PHBV wood fiber composites obtains symbiotic improvement in the mechanical properties. The hybrid green composites showed a pronounced leap of 200% in the Young's and flexural modulus with the dual support of 20 wt.% talc and 20 wt.% the wood fiber in PHBV matrix [18].

1.2 Advantages/ Disadvantages

Natural fiber or bio-composites provide adequate specific strength and modulus while offering several performance advantages over homogeneous Glass Fiber Reinforced Polymer (GFRP) composites including lower density, lower cost, biodegradability, and improved thermal/insulating properties [19,20]. One significant disadvantage of natural fibers is the variability inherent in the material. By harvesting season and region, local sun, rain and soil

conditions, the part of the plant harvested, and the maturity of the crop, the mechanical properties of natural fibers vary [21,22]. Ramesh et al. [23] found that sisal/ jute/glass hybrids exhibited improved tensile strength and modulus compared with jute/glass or sisal/glass hybrids. Boopalan et al. [24] showed that a 50/50 jute/banana FRP exhibited higher tensile strength, flexural strength and impact strength of the single natural fiber composites. Silva et al. [25] showed that sisal and jute fibers could replace glass and carbon fibers in many applications considering availability and cost.

Natural fiber offers several advantages such as excellent mechanical properties, thermal stability, and low processing density [26,27].Bio-binders reinforced with bio fibers showed considerable improvement in tensile properties of bio-composites [28]. It is apparent from work done so far on biodegradable composites that the tensile strength of fully biodegradable composites varied from 20-73MPa and maximum tensile strength 73MPa was recorded when the composites fabricated using PLA reinforced with Hemp and minimum tensile strength was found in Polycaprolactone bio-binder, reinforced with flax fiber [29]. The tensile modulus of bio-composites varied with the addition of different bio binders and bio fibers. The maximum tensile modulus was 20 GPa reported in PLA with sisal fiber and lowest modulus reported in Polycaprolactone bio-binder reinforced was with flax fiber [29].

1.3 Applications

Silk fiber has been used in biomedical applications mainly as sutures by which the silk fibroin fiber is usually coated with waxes or silicone to enhance material properties and reduce

fraying. But in fact, there are lots of confusing questions about the usage of this kind of fiber as there is the absence of detailed characterization of the fiber used including the extent of extraction of the sericin coating, the chemical nature of wax-like coatings sometimes used, and many related processing factors. For example, the sericin glue-like proteins are the primary causes of adverse problems with biocompatibility and hypersensitivity to silk. The variability of source materials has raised the potential concerns with this class of fibrous protein. Silk's knot strength, handling characteristics and ability to lay low to the tissue surface make it famous suture in cardiovascular applications where bland tissue reactions are desirable for the coherence of the sutured structures [30]

CHAPTER II

HIGH STRAIN RATE ANALYSIS WITH SPLIT HOPKINSON PRESSURE BAR (COMPRESSION)

2.1 High Strain Rate Experiment: -

One of the defining features of impacts that occur at velocities sufficiently large to cause inelastic (and mainly plastic) deformations is that most of these deformations arise at high strain-rates. These deformations may also lead to significant strains and high temperatures. Unfortunately, we do not understand the high-strain-rate behavior of many materials (often defined as the dependence $\sigma_f(\varepsilon,\dot{\varepsilon},T)$ of the flow stress on the strain, strain rate and temperature), and this is particularly true at high strains and high temperatures. Some experimental techniques have therefore been developed to measure the properties of materials at high strain-rates. In this section, we focus on those experimental methods that develop controlled high rates of deformation in the bulk of the specimen, rather than those in which high-strain-rates are developed just behind a propagating wave front. The primary experimental techniques associated with the measurement of the rate-dependent properties of materials are described in Figure 2. 1 (note that the stress states developed within the various methods are not necessarily identical). An excellent and relatively recent review of these methods is presented by Field et al. [Figure 2.1].

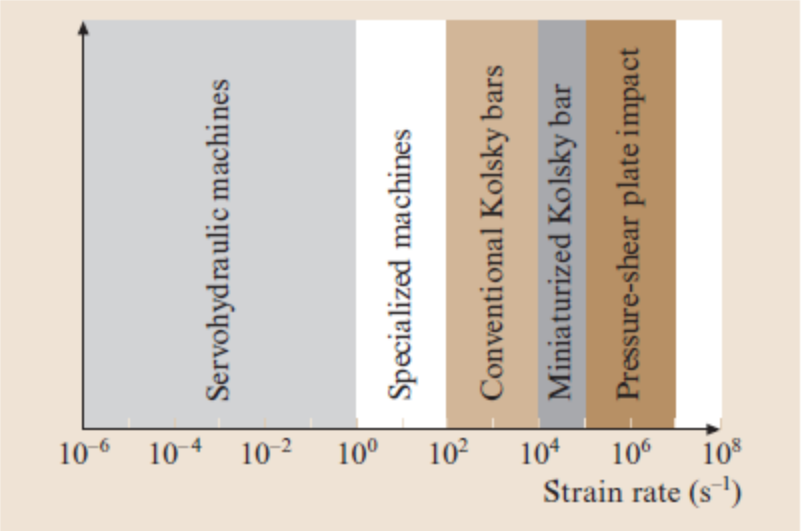

Figure 2.1 Experimental techniques used for the development of controlled high strain rate deformations in materials[38]

For this discussion, strain rates above 10^2 s^{-1} are classified as high strain rates, strain rates above 10^4 s^{-1} are called very high strain rates, and strain rates above 10^6 s^{-1} are called ultra-high strain rates. Conventionally, strain rates at or below 10^{-3} s^{-1} are considered to represent quasi-static deformations, and strain rates below 10^{-6} s^{-1} are in the creep domain. Creep experiments are typically performed at relatively high temperatures, and a variety of specialized machines exist for these kinds of loading; dead loads are often of interest. Quasi-static experiments are typically accomplished through a variety of servo-hydraulic machines, and ASTM standards exist for most of these experiments. Most servo-hydraulic machines are unable to develop strain rates larger than 10^0 s^{-1} repeatable, but some specialized servo-hydraulic machines can achieve strain rates of 10^1 s^{-1}. Finally, the strain rates in the intermediate rate domain (between 10^0 s^{-1} and 10^2 s^{-1}) are extremely difficult to study, since this is a domain in which wave-propagations are relevant and cannot be easily accounted for (however, the strain rates in this domain are indeed of interest to a number of machining problems).

2.2 Fundamentals of Hopkinson bar testing

The split Hopkinson bar test is the most commonly used method for determining material properties at high rates of strain. Significant advancements implemented in the areas of testing techniques, numerical methods, and signal processing have improved the accuracy and repeatability of high strain rate testing. Constant strain rate tests can be performed at strain rates approaching 10^4 s^{-1} relatively easily. In the split Hopkinson bar test, a short cylindrical specimen is sandwiched between two long elastic bars, as shown in Figure 2.2. The bars are made of a high strength maraging steel with diameters less than 0.75" and a length near five feet.

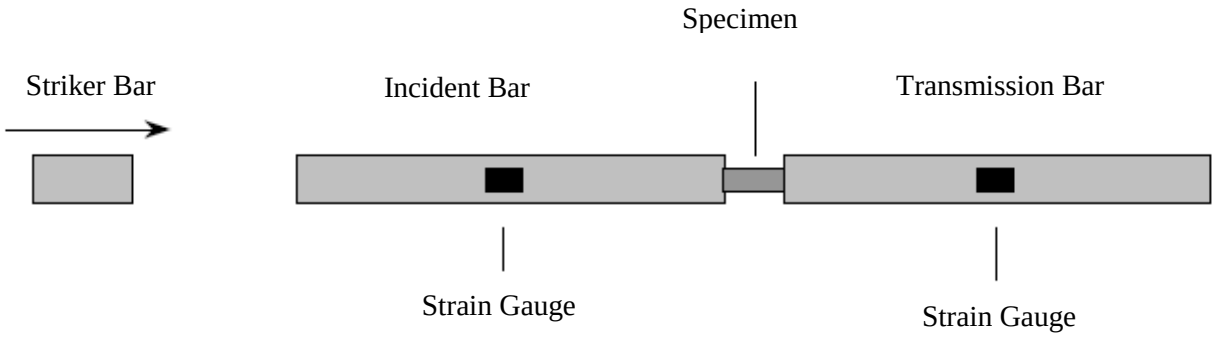

Figure 2.2 Schematic of split Hopkinson pressure bar (SHPB) apparatus[38]

The ends of the pressure bars and specimen are machined flat to enforce prescribed boundary conditions. Striker bar is fired into the end of the incident bar generating a compressive stress pulse. Immediately the following impact, this pulse travels along the bar towards the incident bar-specimen interface at which the pulse is partially reflected into the input bar and partially transmitted through the specimen and into the transmission bar. The reflected pulse is indicated as a wave in tension, whereas the transmitted pulse remains in compression. The strain histories in the incident and transmission bars are recorded by strain gauges mounted on the incident and transmission bar. So long as the pressures in the bars remain under their elastic

limits, specimen stress, strain, and strain rate may be calculated from the recorded strain histories. Under certain deformation conditions, qualified later, only two essential strain pulses need be identified. These are the reflected pulse and the pulse transmitted through the specimen.

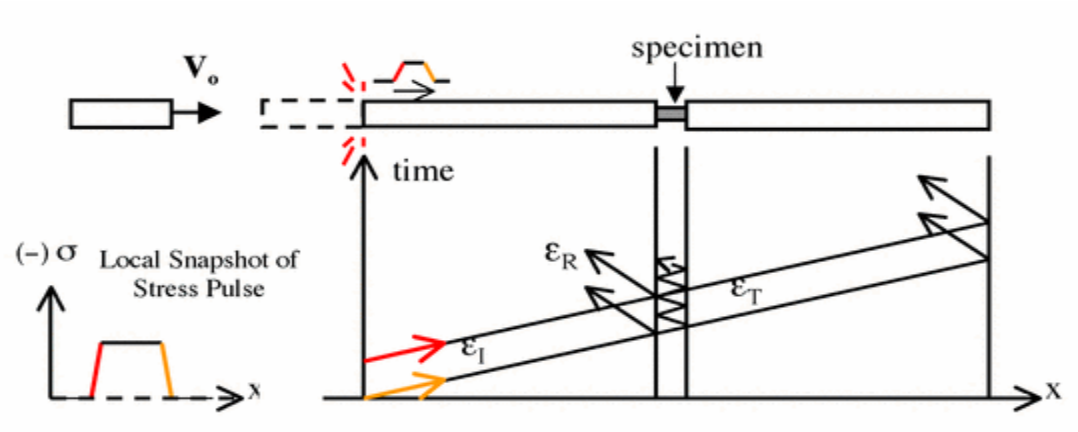

Figure 2.3 Schematic of SHPB with x-t diagram showing the motion in time and 1D space of the compression pulse.[38]

Note: ε_I, ε_R and ε_T are respectively the incident, reflected and transmitted pulses.

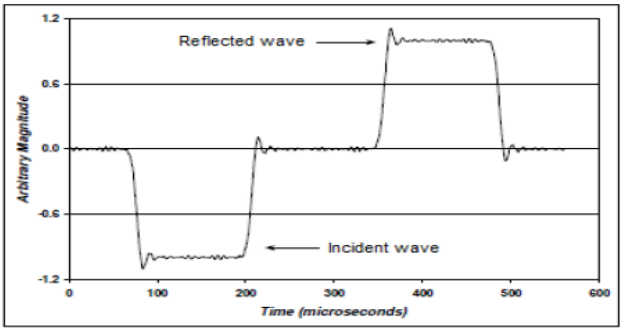

Figure 2.4 Incident and reflective wave

2.3 Theory of Split Hopkinson Pressure bar

The dynamic stress-strain, strain rate an energy absorption can be obtained from the incident, reflected and transmitted strain pulse. From mass conservation, if ε_i, ε_r and ε_t are respectively the incident, reflected and transmitted pulses and subscript 1 & 2 are the two ends of the specimen, the displacement at the ends of the specimen is given by:

$$u_1 = \int_0^t C_0 \varepsilon_1 dt \tag{1}$$

$$u_2 = \int_0^t C_0 \varepsilon_2 dt \tag{2}$$

Where C_0 is the wave velocity in the Hopkinson bars, in terms of the incident, reflected and transmitted pulses,

$$u_1 = C_0 \int_0^t (\varepsilon_i - \varepsilon_r) dt \tag{3}$$

$$u_2 = C_0 \int_0^t \varepsilon_t dt \tag{4}$$

Where stresses and strains assumed positive in compression. The average strain in the specimen is:

$$\varepsilon_s = \frac{u_1 - u_2}{L} \tag{5}$$

Or in terms of the strain pulses:

$$\varepsilon_S = \frac{C_0}{L} \int_0^t (\varepsilon_i - \varepsilon_r - \varepsilon_t)\, dt \tag{6}$$

Where L is the length of the specimen. From momentum conservation, the forces at the end of the specimen obtained from:

$$P_1 = EA(\varepsilon_i + \varepsilon_r) \tag{7}$$

$$P_2 = EA\,\varepsilon_t \tag{8}$$

Where E and A are Young's modulus and cross-sectional area of the Hopkinson bars. The average force is calculated from:

$$P_{av} = \frac{EA}{2}(\varepsilon_i + \varepsilon_r + \varepsilon_t) \tag{9}$$

If it is assumed that $P_1 = P_2$, that is forces are equal at both ends of the specimen, then from (7) and (8):

$$(\varepsilon_i + \varepsilon_r) = \varepsilon_t \tag{10}$$

$$\varepsilon_S = \frac{C_0}{L}\int_0^t (\varepsilon_i - \varepsilon_r - \varepsilon_r - \varepsilon_t)\,dt \tag{11}$$

$$\varepsilon_S = \frac{-2C_0}{L}\int_0^t \varepsilon_r\,dt \tag{12}$$

$$P_{av} = EA\varepsilon_t \tag{13}$$

For the specimen of cross–sectional area A_s, the stresses and strain rate in the specimen become:

$$\sigma_s = E\frac{A}{A_S}\varepsilon_t = K_1\varepsilon_t \tag{14}$$

$$\dot{\varepsilon_s} = \frac{-2C_0}{L}\varepsilon_r = \varepsilon_r \tag{15}$$

K_1 and K_2 are the stresses and the strain rate multiplying factors for a given specimen and, the setup. Hence, only the transient strain data is required to be recorded. By using recorded data and equations 14 and 15, the transient stress and strain rate can be calculated. Strain rate data can be calculated. Strain rate data is then integrated to get the strain versus time data. Then by superimposing with the stress versus time data, the transient stress – strain data is obtained. To calculate the absorbed energy density (energy/unit volume), the following data is used:

$$U_a = \frac{1}{2}\int_0^t \sigma_{(t)}\varepsilon_{(t)} \quad (16)$$

The absorbed energy is then calculated by multiplying the above quantity obtained with the volume of the sample.

There some assumptions in the theory of SHPB are [7]

1. Bars are always elastic.
2. One dimensional planar wave in the bars.
3. Uniaxial stress state in the specimen.
4. Uniform stress state in specimen i.e. negligible wave propogation effect in specimen.
5. Friction and inertia effect in the specimen is minimum.
6. The specimen is not compressible.

2.4 Design considerations of SHPB

Like many other apparatus, there are certain criteria associated with the design of SHPB to get good experimental results. Few of them are listed below:

1. Vibration free: SHPB apparatus should be vibration free. A vibration table or bench can be used for precise measurements.

2**. Friction free:** Friction between bars and the brackets used to support bars should be minimized for better results. Friction between specimen and bar ends also need to bar minimized.

3. Alignment: Alignment of striker bar with incident bar, incident bar with transmission bar and specimen with incident and transmission bar is the most crucial aspect of the SHPB. Specimen and surfaces ae required to be parallel (within 0.5%).

4. Dimensions of the bar: Incident and transmission bar should be long (L/D>> 20) and straight so that the radial and shear components of the stresses are negligible. Incident bar should be at least twice the length of the striker bar. Transmission bar should be longer than the striker bar.

5. The material of the bar: Bar should always be with the elastic range. Metallic bars like steel are strongly recommended due to large yield stress.

6. Strain Gages: Precision strain gages should be employed. Strain gages should be located at least ten times of diameter of bar diameter from the end.

7. Signal conditioner/amplifier: Wheatstone bridge is preferred circuit. The frequency response of the electrical circuit should be sufficient.

8. Data recorder: Oscilloscope or high-speed acquisition card with high sampling rate, high resolution (8 bit or more), and high bandwidth/frequency response should be used. It should have sufficient data storage capacity.

2.5 Design overview of Compression and tensile SHPB:

Schematic of compression and tensile SHP is shown in Figure 2.5 & 6 The SHPB apparatus works on compressed air generated in a compressor. This compressed air is stored in an air chamber at the pressure on which experiments are to be performed. The solenoid valve is used to expand the compressed air into the barrel which pushes the striker bar. Two diametrically

opposite strain gauges each on incident and transmission bar are mounted in one arm of the whetstone bridge to form a quarter bridge configurations. Incident and reflected waves from the incident bar and transmission wave from transmitted bar strain gauges are recorded to obtain the material response under dynamic conditions.

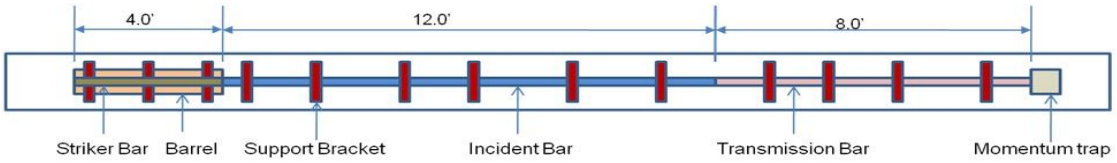

Figure 2.5 Schematic of compression Split Hopkinson bar at The University of Mississippi

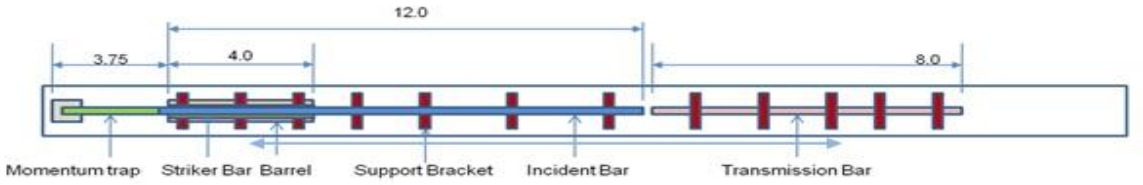

Figure 2.6 Schematic of tensile Split Hopkinson bar (SHPB) at The University of Mississippi

Figure 2.7 Split Hopkinson bar at The University of Mississippi

2.6 Parts of Split Hopkinson pressure bar (SHPB):

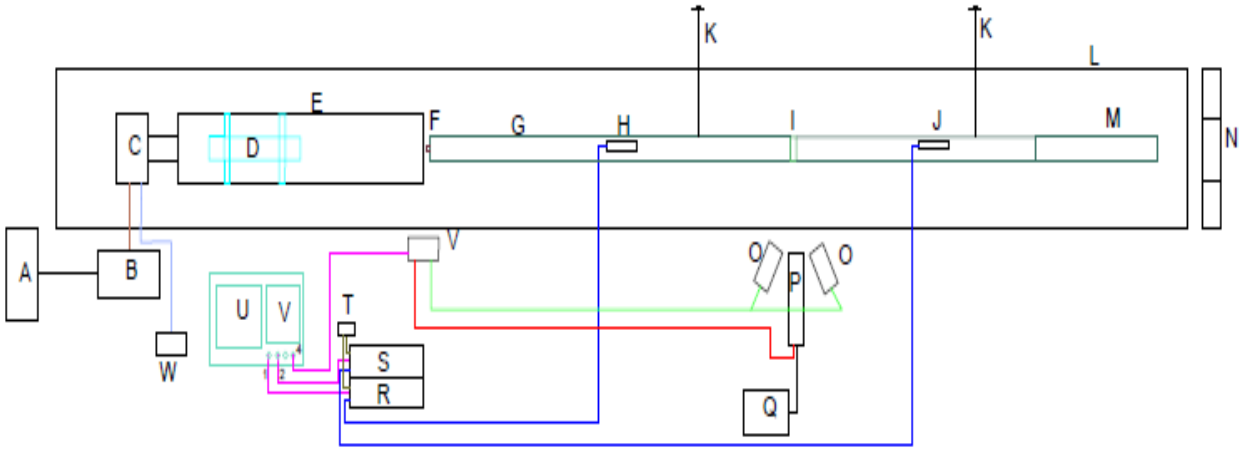

Figure 2.8 Schematic of Split Hopkinson bar (compression) at The University of Mississippi

Nomenclature:

A – Pump

B – Compressor unit

C – Solenoid valve

D – Striker bar

E – Barrel

F – Pulse shaper

G – Incident bar

H – Strain gauge 1

I – Specimen

M – Momentum trap bar

N – Momentum trap putty

O – Strobe

P – Camera

Q – Computer

R – Signal conditional amplifier 1

S – Signal conditional amplifier 2

T – Wheatstone bridge

U – Waveform display on oscilloscope

J – Strain gauge 2

K – Electrically grounded

L – SHPB base

1. **The base of SHPB (L): -** A robust I - beam with a height of 24” (609.6 mm) was used as the base of SHPB as shown in Figure 5. Stainless steel liner was mounted on top surface of the beam for proper leveling and smoothness.

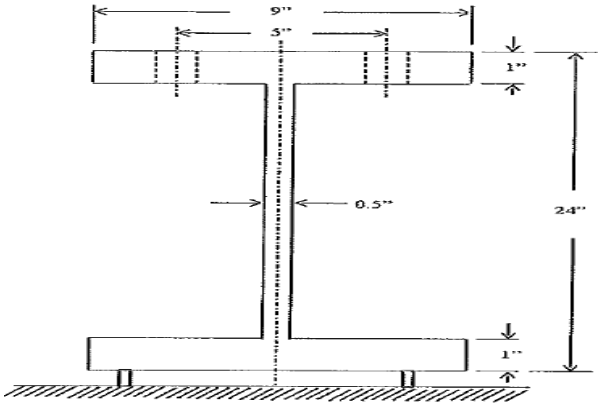

Figure 2.8 Schematic of I - Beam

2. **Pump with compressor unit(A & B): -** A pump of 6 gallons and with a capacity of 150 psi and air compressing chamber of 150 psi is installed on I – beam.

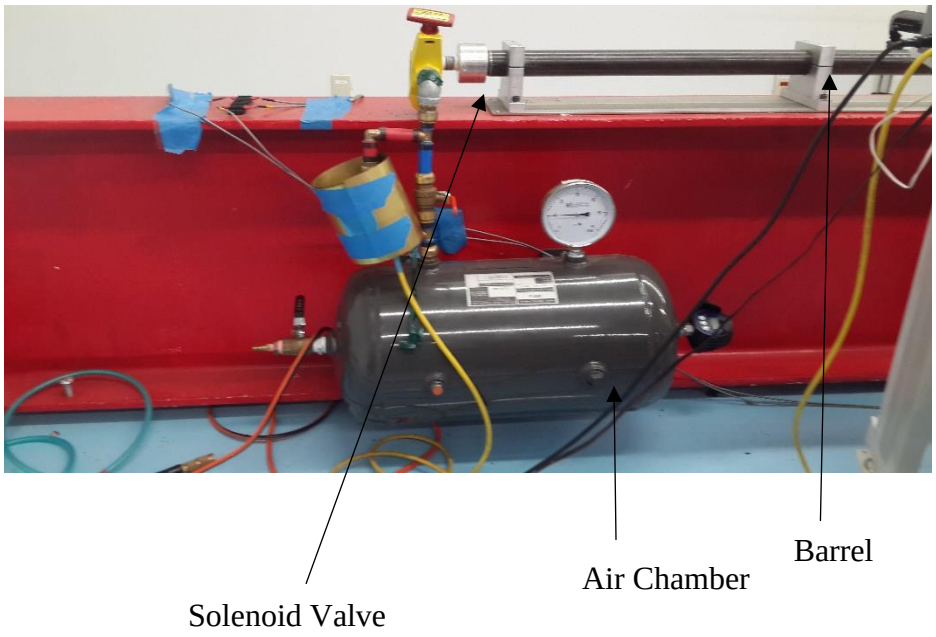

Figure 2.9 Solenoid Valve, compression chamber and barrel of compression SHPB

3. **Barrel for striker bar (E): -** 48" (1220 mm) long barrel with inside diameter of 1.5" (38.1 mm) was used to house the striker bar as shown in Figure 2.9.

4. **Solenoid valve (C): -** Solenoid valve was used to control the flow of compressed air from air chamber to barrel as shown in Figure 2. 9

5. **Striker bar (D): -** Solid stainless steel (Aquanox 19) having diameter of 0.75" (19.75 mm) and the length of 18" (457.2 mm) was used as the striker for compression SHPB. In case of tensile SHPB, a hollow striker bar with inside diameter of 0.75" (19.05 mm) and outside diameter of 1.25" (31.75 mm) and length of 18" (457.2 mm) was used as it is supposed to slide over the incident bar as shown in Figure 2.10. A plastic bush was used in between striker bar and barrel to avoid metal to metal contact.

Figure 2.10 Striker bar

6. **Incident and transmission bar (D): -**Solid stainless steel (Aquanox 19) of diameter ¾" (19.05 mm) with the length of 144" (3567.6 mm) respectively were used for the incident and transmission bars. For tensile SHPB, end of the bar was threaded to put a sleeve of outside diameter 1.75" (44.5 mm) on which striker bar will provide an impact as shown in Figure 2. Mating ends of incident and transmission bars were threaded to put an adaptor for mounting specimen in the tensile SHPB as shown in Figure 2.

7. **Momentum trap (M): -** Momentum trap was used to trap the motion of the bar after the event is over; at the end of the incident bar in tensile SHPB as shown in Figure 2. 5 & 6. Momentum trap was initially mounted on I – beam but later were isolated because it will transfer the energy to the beam and may cause the change in alignment of the bars.

8. **Strobe (O):** The basic function of the strobe is to illuminate the specimen. A strobe (Figure 2. 11) from HADLAND of 1000 Watt light intensity used in compression SHPB. Furthermore, the longest rise time for the strobe to achieve for Full lighting intensity is 120 μs (microseconds).

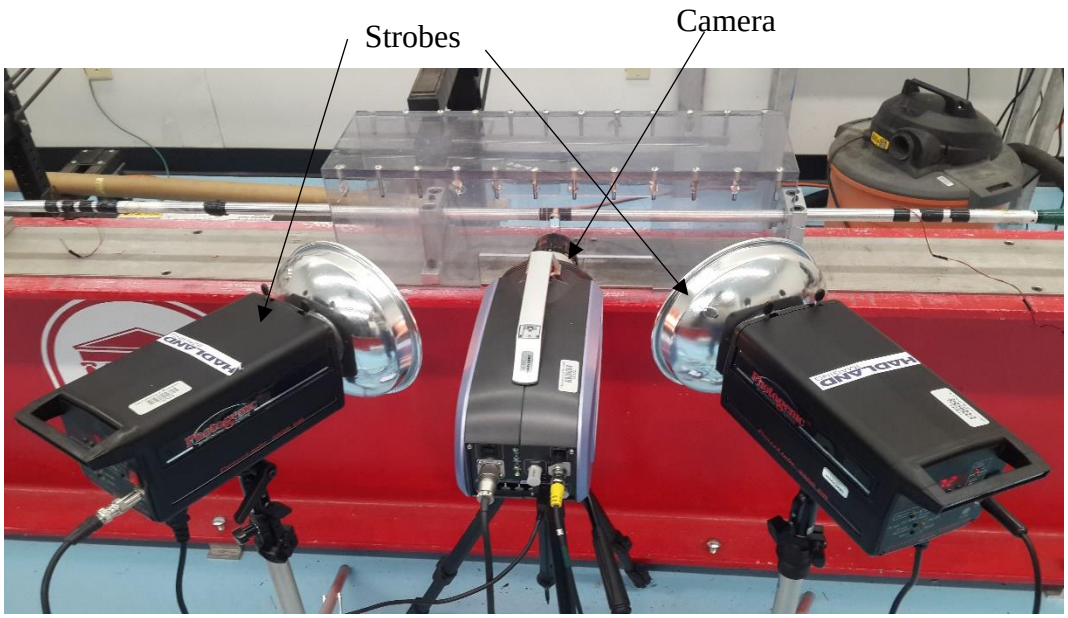

Figure 2.11 Camera and strobes

9. **Camera (P):** High digital photography is done by the camera (Figure 2. 11) during the experiment. Camera has maximum speed of 1 million frames per second and the minimum is 33 frames per second. It has fix resolution of 312*260 pixels. It can only record 102 frames at any speed.

10. **Strain gauges (H & J);** - The primary function of strain gauge is to measure the deflection experienced by the rod and to get the Voltage vs Time history in oscilloscope from incident bar and transmission bar. Two diametrically opposite strain gauges of 350 Ω (Ohm) resistance were mounted on each bar and connected to series as shown in Figure 2. 12.

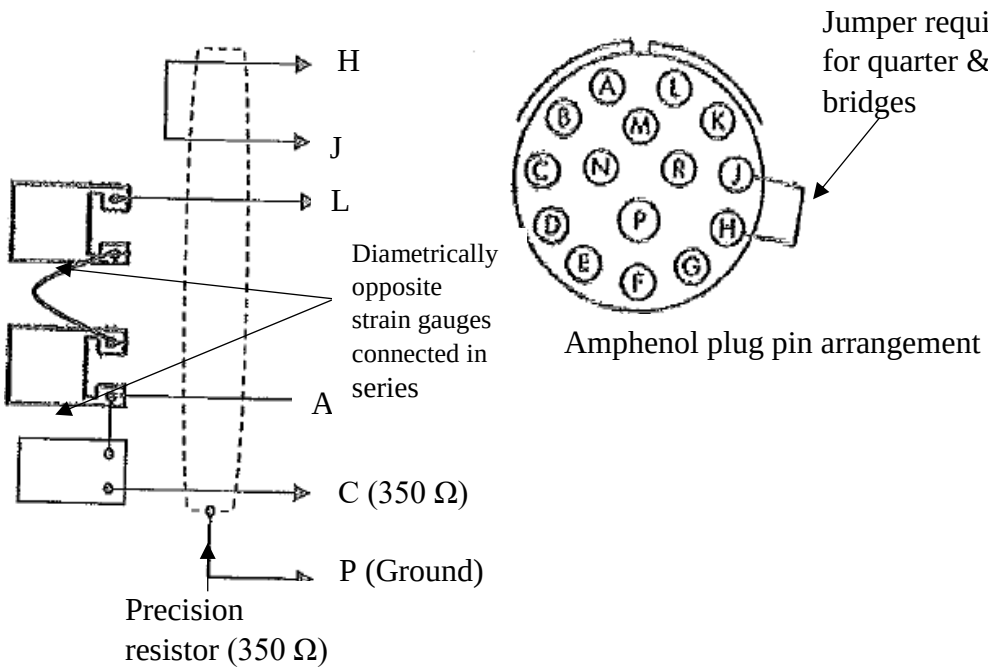

.

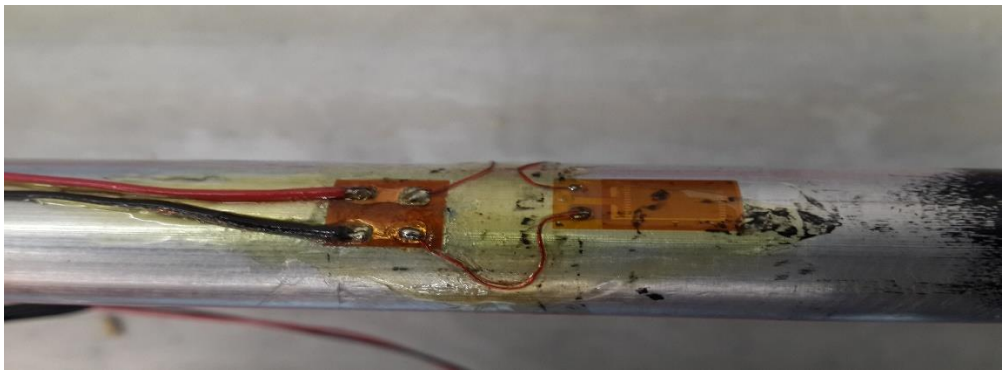

Figure 2.15 Strain gauges mounting on SHPB

11. Signal conditioner: - Model 2310 B from Vishay Mismeasurements was used to form whetstone bridge configuration. Both strain gauges were connected in series to one arm of the Wheatstone bridge to make quarter bridge circuit. Schematic of circuit diagram is shown in Figure 2.12.

Figure 2.13 Signal Conditioner 2310 B front panel

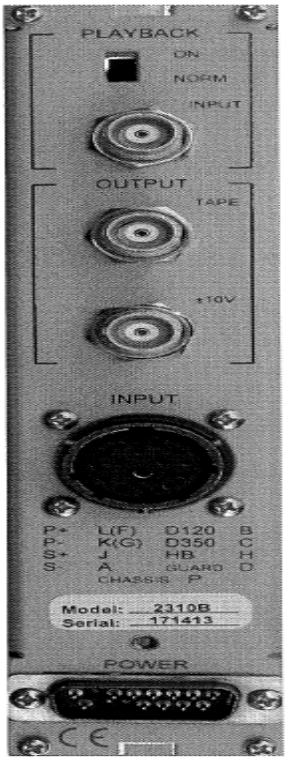

Figure 2.14 Signal Conditioner 2310 B rear panel

Differential pre-amplifier: - Differential preamplifier model AD400A from Tektronix was used which allows direct oscilloscope measurements of very low amplitude voltages and signals which are not ground referenced.

12. **Digital Oscilloscope: -** Digital oscilloscope model TDS 3014C from Tektronix was used to record signals.

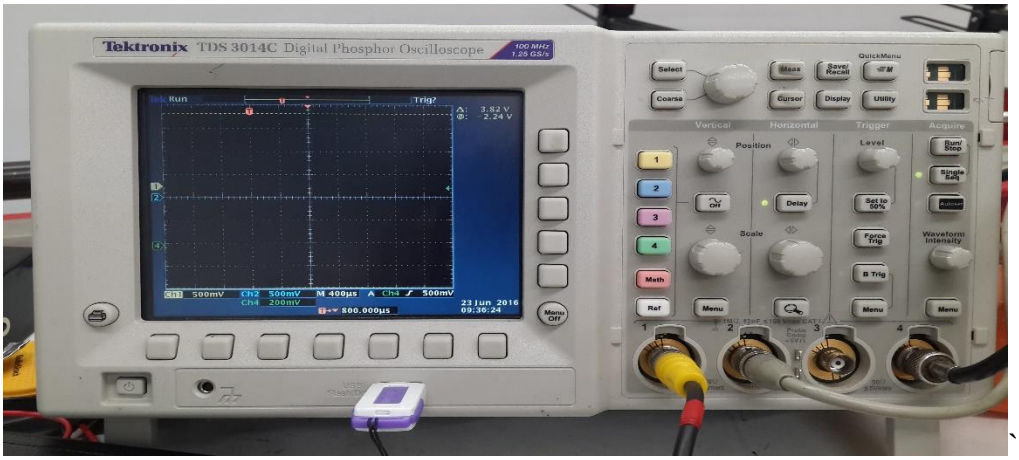

`1

Figure 2.16 Oscilloscope used for recording data

13. **TTL Box: -**TTL box is used to trigger the camera and strobe, for simultaneous lighting and camera footage. It uses sound to trigger. It has voltage setting for the strobe is 0.5 V and camera is 5V.

2.6 Instructions for Performing a Split Hopkinson Pressure Bar Experiments

(Standard Operating procedure)

Compression SHPB:

Specimen preparation:

1. The specimen dimensions should follow the below relation:

$$\frac{L}{D} = \sqrt{\frac{3\upsilon}{4}}$$

where L is the length, D is the diameter and υ is the Poisson's ratio of the specimen.

2. Make sure the faces of the specimen are parallel and flat (use step collet while machining metal specimens to get parallel faces). The diameter of the specimen after the test should be smaller than the diameter of the pressure bars.

Selecting the bar:

1. Determine the impedance (ρcA) of the specimen.

   where ρ is the density, c $\left(c = \sqrt{\frac{E}{\rho}} \right)$ is the wave speed and A is the area.

2. Then select the pressure bars (steel or Aluminum) closer to the impedance of the specimen.

   Note: The basic thumb rule is that usage of steel bars for the harder materials (metals etc..) and Aluminum bars for the softer materials (polymers, foams etc..).

3. After the pressure bars are selected, make sure the end faces of the bars are flat and parallel.

4. Align the pressure bars and striker on the mounting frame.

2.7 Experimental procedure:

(a) Give all required connections. Connections include: Connect the BNC cables from the amplifier to the oscilloscope. Check the right channels and connect them. Make sure the amplifier and oscilloscope are grounded. Turn ON the amplifier and oscilloscope.

(b) The excitation voltage and gain are set to 10V and 100 respectively. Turn the reset switch ON for all the four channels.

(c) Check the resistance on the strain gauges and they should read around 350 ohms.

(d) Set the voltage levels, trigger position, data duration time (2ms-4ms), for all the three channels in Oscilloscope. These values depend on the experiments.

(e) Balance the Wheatstone bridge for all the four channels by turning the reset button.

(f) Check whether the bars are well aligned or not, and also the projectile should be well aligned to the impact end of the incident bar.

(g) Then make sure that the bars are moving freely, if not adjust the screws of the clamps.

(h) Clean the interfaces of the bar and the projectile.

(i) Push the projectile to the end of the barrel of pneumatic assembly with a rod.

(j) Measure the dimensions of specimen. Dimensions include: diameter and thickness.

(k) Select the striker depending on the strain rate you are trying to get. You can vary strain rate by using different pressures and different striker bars. Make sure the pulses are not getting overlapped. If the pulses are getting overlapped, use the shorter striker bar. (Thumb rule: The longer the striker, the lower the strain rate. The higher the pressure, the higher the strain rate).

(l) In addition to the above point the strain rate depends upon the geometry of the specimen. Thinner the specimen, more strain rate would be experienced by the specimen

(m) Sandwich the specimen between the bars and align the specimen with respect to bar center.

(n) Place the pulse shaper at the impact end of the incident bar with a thin layer of petroleum gel and align it with respect to bar center. Here (at the University of Mississippi) pulse shapers of copper are used. Equilibrium stress state is achieved because of the pulse shaper.

(o) Fill the air thank with air from compressor until required pressure is achieved in the pressure gauge

(p) The oscilloscope should be made ready to capture the signal from strain gauge and triggering symbol from TTL box.

(q) Once again, ensure that the specimen is well aligned between the bars and verify the status of the trigger hold before pressing the solenoid valve release button.

(r) Press solenoid valve control box button to release the projectile.

(s) Save captured voltage pulses onto a USB drive for further analysis of the data.

(t) After the experiment is completed, turn off the cylinder and make sure all the left over compressed air in the air cylinder is released.

(u) After the data is transferred from the oscilloscope to USB drive, verify that in your computer and turn off the amplifier and oscilloscope.

2.8 Example

Testing of 4%MDI over compressed under high strain rate using, split Hopkinson bar.

Table1: Kind of Wood based bio-composites

No.	Type of wood based bio-composite	Heating time	Compression pressure	Ram pressure (psi)	Force (lb_f)
1	4% MDI 4100 psi (ram pressure) with 2x more material	140 seconds	1523.20 psi	3400	804248.00

In this experiment, pulse shaper was placed between the incident bar and the striker bar, so as when the striker bar strikes the incident bar the pulse shaper would come in between. The specimen is placed between the incident bar and the transmission bar and then the Striker bar is launched impacting the pulse shaper and incident bar. Three sample of each type of wood were tested. The high strain rate compression experienced by each kind of wood was recorded by high speed cameras. Different strain rates were obtained by varying pressure of the compressed air in Hopkinson bar. They were 10 psi, 15 psi, 20 psi. Figure 1 shows a schematic diagram, of SPLIT HOPKINSON PRESSURE BAR.

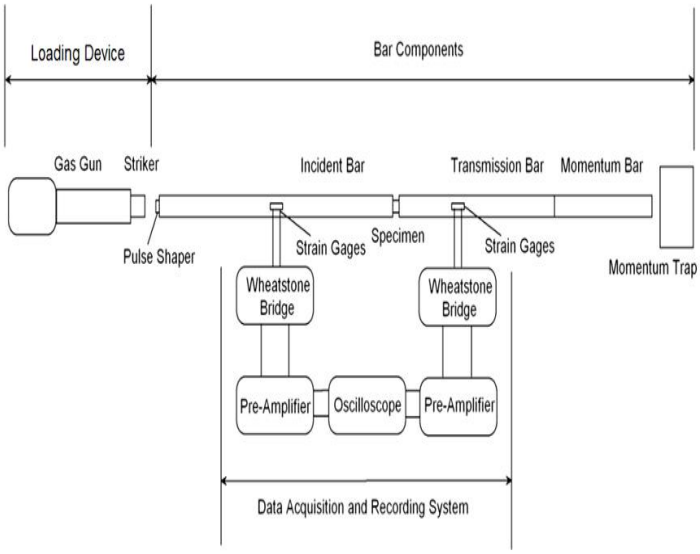

Figure 2.17 A general Kolsky compression bar apparatus

The following results were obtained from the experiment carried out using SHPB using above procedure

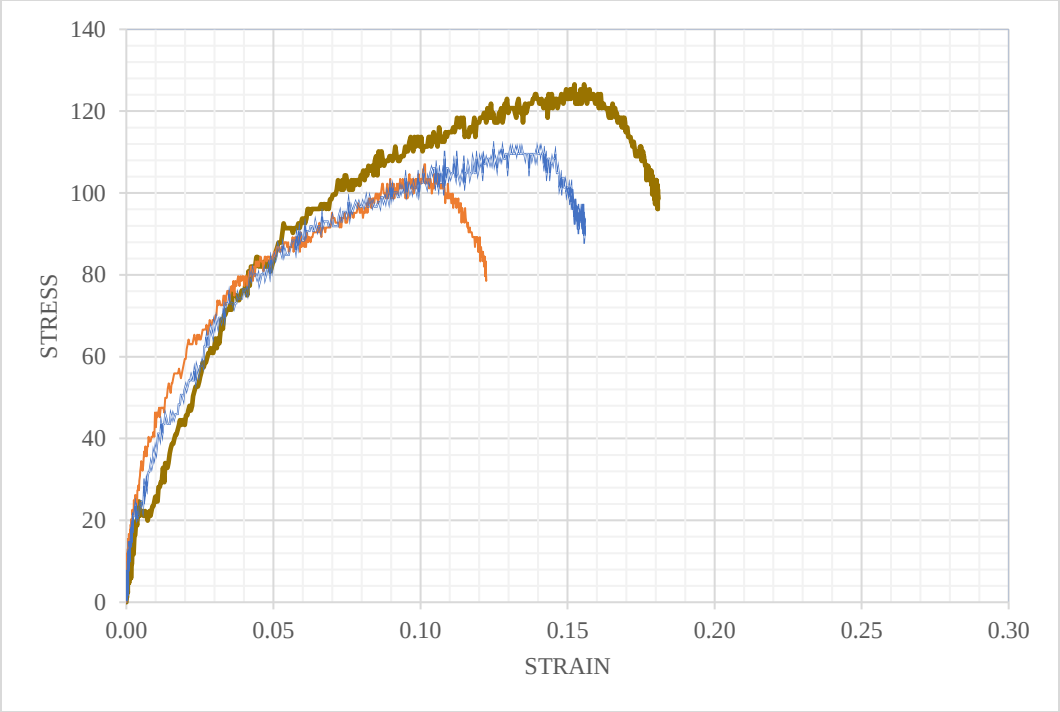

Figure 2.18 Sample Stress-Strain curve

The above results were obtained from SHPB for 4%MDIOverCompressed and it shows high strain rate dependency

- When the strain rate of the specimen is increased, the compressive strength increases
- Stiffness increases
- Strain to failure increases

CHAPTER III

DYNAMIC RESPONSE OF WOOD-BASED BIOCOMPOSITIES UNDER HIGH-STRAIN RATE COMPRESSIVE LOADING

3.1 Introduction

This research focuses on the results obtained from a split-Hopkinson pressure bar (SHPB) experiment performed on several wood-based bio-composites. Characterizing the material behavior at a high strain rate is an important aspect. Afrough et al found the behavior of pultruded glass-graphite/epoxy hybrids under transverse high-strain rate compression loading. Their research found that failure of specimens loaded along transverse direction was dominated by matrix failure. Their study also showed that the ultimate compressive strength was marginally increased by including a higher percentage of graphite[31]. To safely transport nuclear waste and toxic matter, it is required that the material be protected from dynamic loading situations. Wood can be used for such applications. They studied the response of dry maple wood under a high-strain rate compressive impact load. The deformation of the maple specimen was found to be a linear function of energy absorption [32]. Daryadel et al found that the dynamic response of four (borosilicate, soda lime, starphire, and fused silica) commercially available glasses was studied under high-strain rate compressive loading. The results showed that the compressive strength was very sensitive to strain rate, whereas the stiffness remained constant [33]. Bragov and Lomunov obtained dynamic deformation diagrams for pine, birch, and lime using a SHPB.

They found that the deformation diagrams were nonlinear and differ in their loading and unloading brunches. It was also found that the stress values resulted in cracking and spallation [34].

Resources from forests are a major asset to Mississippi and the southeastern United States. Around 19.7 million acres (65%) of the total land area of Mississippi is covered by forests[35] . Thus, developing wood-based products is an important aspect when wood is produced in such a large quantity. New wood-based bio-composites were developed in collaboration with the Department of Sustainable Bioproducts, Mississippi State University. Nine different kinds of wood-based bio-composites were produced by combining various amount of methylene diphenyl diisocyanate (MDI), corn starch (CS), and microcrystalline cellulose (MCC) for various compression periods and various compression pressures. Extensive research has been done in the area of bio-composites because this area has many advantages including the low manufacturing costs involved in producing the final products and producing highly valued products from low-value material. Producing biodegradable products has become a necessity due to petroleum-based products being a finite resource and having more potential to harm the environment. Bio-composites are beneficial because the disposition of the biofibers is not complex and they are natural organic products, which do not pose a biohazard compared with other conventional available fibers. The density of the bio fibers is lower when compared with glass fibers, and they also have thermal insulating and acoustic properties (because of their hollow tubular structure). In this research, the high stain rate compression behavior was studied for nine different bio-composite samples. An SHPB [36-38] was used to obtain the dynamic behavior of different bio-composite samples under high-strain rate compressive loading. A high-speed camera was used to capture the behavior of all the wood configurations under the three

loading conditions. The ultimate goal of the research was to replace conventional construction materials with these types of bio-composites, which have improved properties.

3.2 Materials

The dynamic response under high-strain rate compression was studied for nine different kinds of wood-based bio-composites as shown in Table 3.1. Three replicates of the specimens were tested. The original panel formed from the material measured 508 mm × 559 mm. Specimens were then cut from the center of this panel and measured approximately 12.7 mm × 12.7 mm × 6.7 mm. Table 3.1 displays the nine different wood-based bio-composite compositions tested. The total water content in each mat before being pressed was approximately 6 wt%. The percentages shown in Table 3.1 refer to the solids content in the panel, with the remaining percentage being southern yellow pine. Pure cotton was processed into MCC using methods outlined in a previous study using an HCl solution at 85°C and continuous stirring for 1.5 h [39] Pure CS was obtained and used for panels 4-8.

Table 3.1. Nine samples dynamically tested with the Split Hopkinson Bar procedure.

No.	Type of wood based bio-composite	Curing time (seconds)	Compression pressure (psi)
1	4% MDI	140	1294 psi
2	4% MDI, 1% MCC	140	1332 psi
3	4% MDI, 2% MCC	140	1028 psi
4	2% MDI, 2% CS	140	1256 psi
5	2% MDI, 4% CS	140	1332 psi
6	4% MDI, 2% CS	140	1332 psi
7	4% MDI, 4% CS	140	1218 psi
8	4% MDI, 4% CS	600	1370 psi
9	4% MDI HP (high pressure) with 2x more material	140	1523 psi

3.3 Equipment and Experimental Procedure

A Dieffenbacher hot press system (450 ton, 34″ × 34″, PressMAN system, Alberta Research Council, Edmonton, Alberta, Canada) located at the Sustainable Bio products Laboratory at Mississippi State University was used to create the panels used in this study. The ram had an area of 201.1 in^2, a 40-HP motor and a pump size of 71 mL/rev. This hot press with steam injection capability was coupled with the Alberta Research Council's Pressman operation and monitoring software. The same amount of material was used to form the panels (except twice the amount of material was used to produce panel no 9), and the press was programmed to produce a panel with a particular thickness (6.35 mm).

A Kolsky bar or SHPB was used to obtain the dynamic behavior of the composites under three ranges of strain rate (varying from 560 to 1568 s^{-1}). The experiments were carried out at the Blast and Impact Dynamics lab, University of Mississippi, a schematic of the same is shown in Figure 3.1. Aluminum bars with a 19.02-mm diameter and an annealed copper pulse shaper were used between the striker and the incident bar to ramp up the incident pulse and slow down the rate of loading. This method allowed the samples to be dynamically loaded at an equilibrium stress state. A pulse shaper was placed between the incident bar and the striker bar, so when the striker bar would strike the incident bar, the pulse shaper would come between the striker and the incident bar. The specimen was placed between the incident bar and the transmission bar and then the striker bar was launched to impact the pulse shaper and incident bar. Three replicates of each type of bio-composite were tested. The high-strain rate compression experienced by each kind of composite was recorded by high-speed cameras. Different strain rates (varying from 560 to 1568 s^{-1}) were obtained by varying the pressure of the compressed air in the Hopkinson bar.

The pressures used for this purpose were 10, 15, and 20 psi. Figure 3.1 shows a schematic diagram of the SHPB.

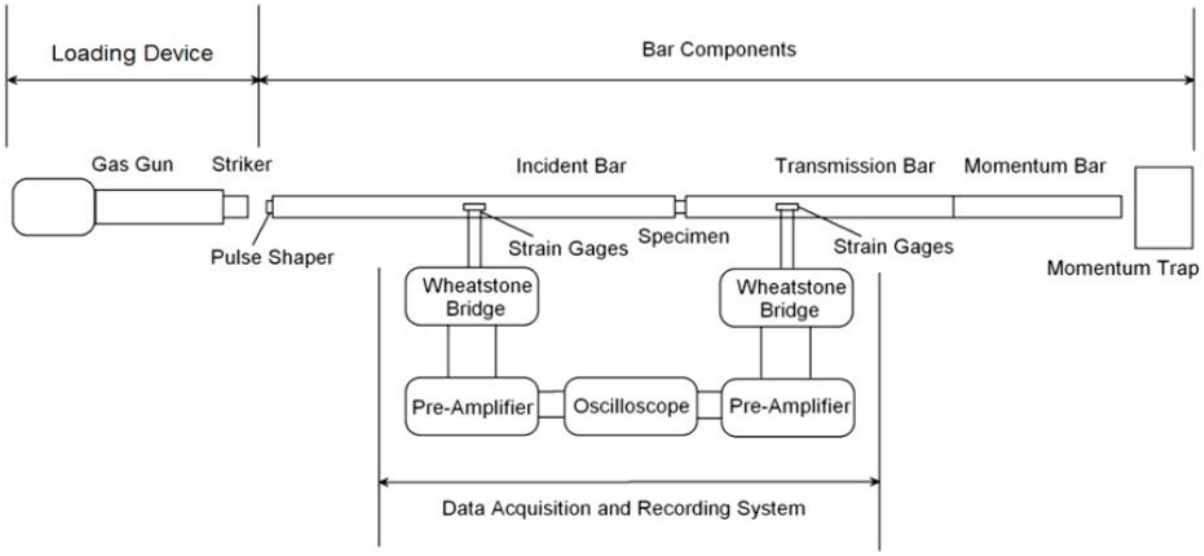

Figure 3.1. Split Hopkinson Bar (Kolsky) diagram – device located at the University of Mississippi [38].

3.4 Experimental Results and Discussion

The dynamic relationship of the wood composite samples at 10 psi (560-1053 s^{-1}, was the range of strain rate achieved under this pressure) is shown in Figure 3.2. It was observed that the maximum strain was 0.30. Here it was observed that the 4%CS2%MDI140S sample had the lowest yield strength and the 4%MDIHP140S sample had the highest yield strength. When comparing samples which were formed under the similar pressure, the 4%CS4%MDI600S sample had the highest yield strength. When comparing samples, which were formed under the *similar* pressure and curing time, the 2%CS2%MDI140S sample had the highest yield strength. These results varied when the strain rate was changed.

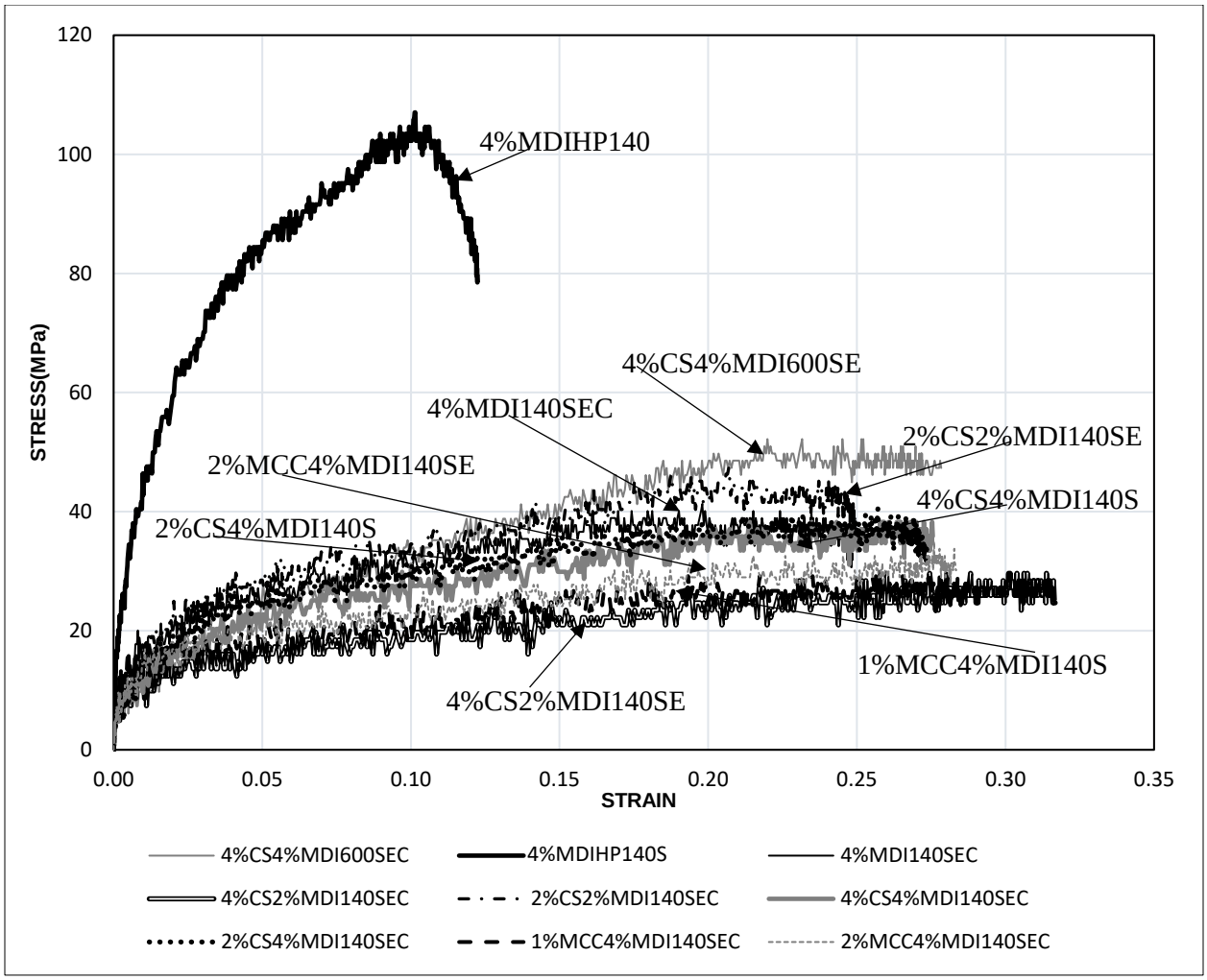

Figure 3.2- Dynamic Stress-Strain curve of wood based bio-composites at 10 psi (Strain rate from 560 s^{-1} to 1053 s^{-1})

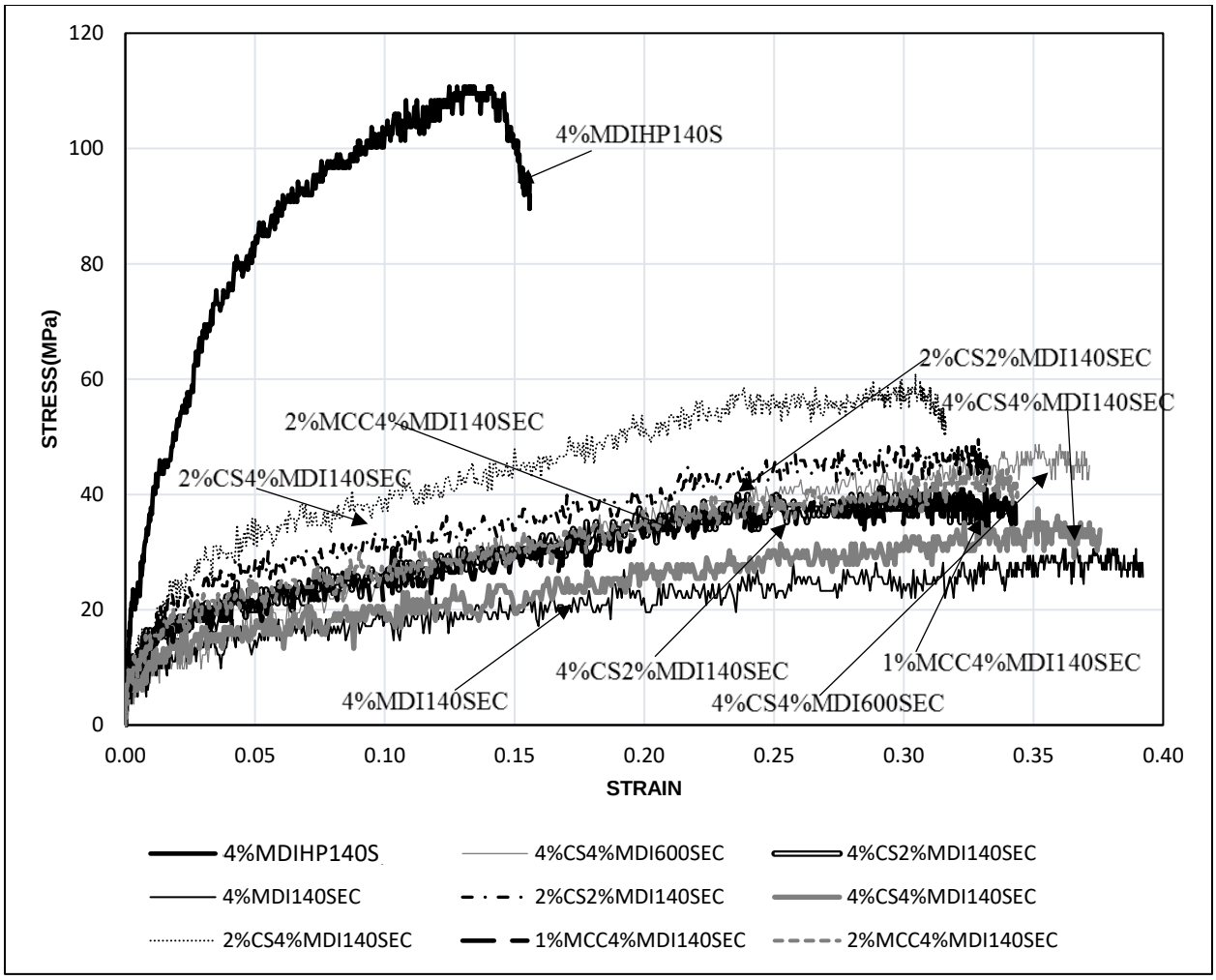

Figure 3.3- Dynamic Stress-Strain curve of wood based bio-composites at 15 psi (Strain rate from 727 $s^{-1}$to 1380 s^{-1})

Figure 3.3 shows the dynamic stress-strain curve of the wood-based bio-composites at 15 psi (727-1380 s^{-1}, was the range of strain rate achieved under this testing pressure). This graph shows that the 4%MDI140S sample had the lowest yield strength, and the trend of the stress-strain curve differed slightly in comparison with the stress-strain curve at 10 psi. The 4%MDIHP140S sample still showed the highest yield strength. Here the maximum strain increased to 0.39. When comparing samples, which were formed under the *similar* pressure and

curing time, the 2%CS4%MDI140S sample had the highest yield strength. The 4%MDI140S sample had the largest strain compared with other wood samples.

Figure 3.4 shows the dynamic stress-strain curve of the composites tested at 20 psi (766-15837 s^{-1}, was the range of strain rate achieved under this pressure). The sample that was formed under the highest pressure (4%MDIHP140S) had the highest yield strength, whereas the sample containing 1% MCC had the lowest yield strength. When comparing samples, which were formed under the *similar* pressure and curing time, the 2%CS2%MDI140S sample had the highest yield strength.

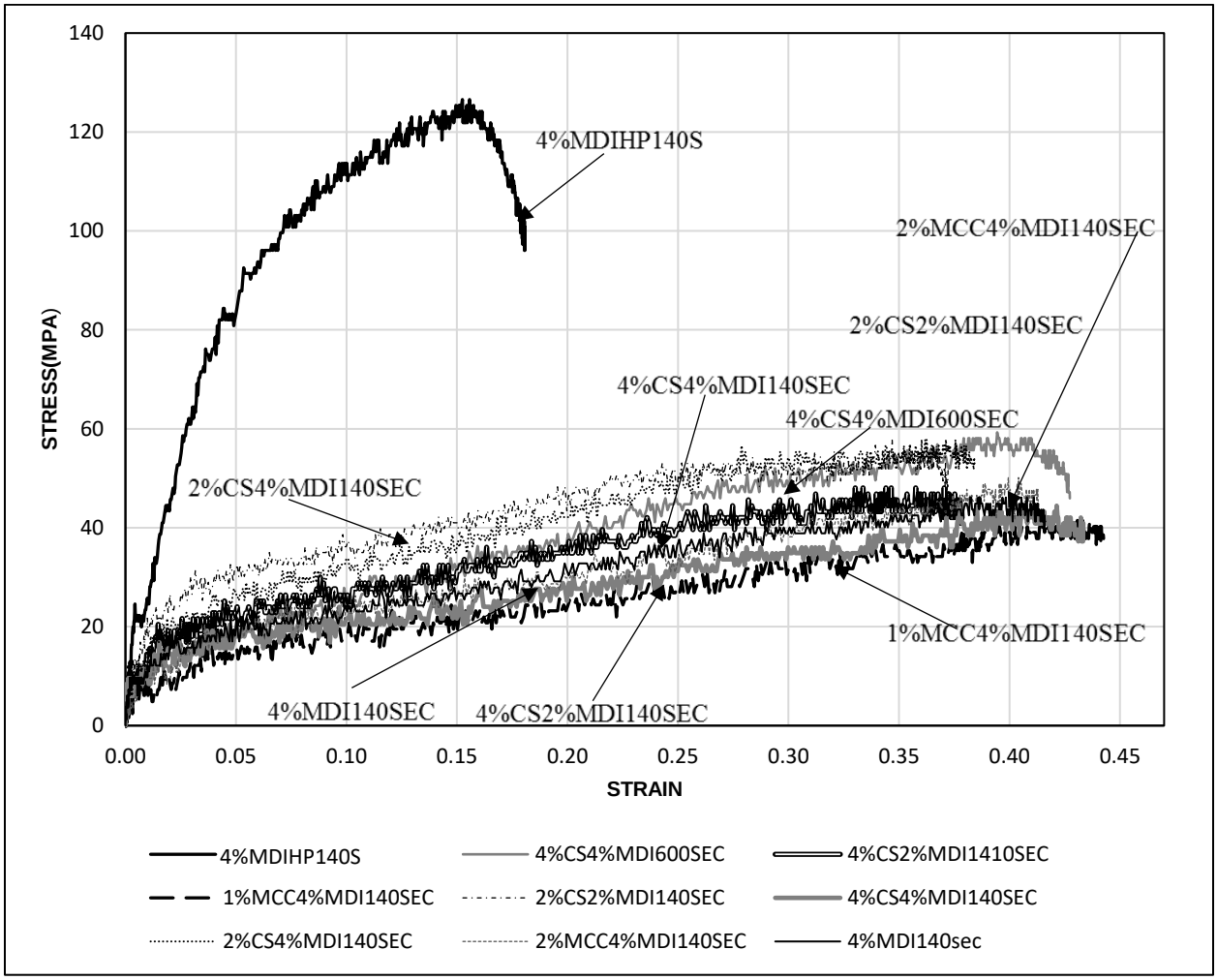

Figure 3.4- Dynamic Stress-Strain curve of wood based bio-composites at 20 psi (Strain rete from 766 s^{-1} to 1587 s^{-1})

The samples containing CS consistently show a higher yield strength when compared with samples containing MCC. The stress-strain relationship shows that each sample (except for the 4%MDIHP140S) is highly plastic. This result shows that each of these samples has an incompressibility property of plastic deformation and is highly incompressible. As these samples were being plastically deformed, they experienced a shape change when loading was experienced because plastic strain was responsible for their shape change. However, the 4%MDIHP140S sample was shown to be highly elastic. High elastic strain in the 4%MDIHP140S sampled induced a volume change, so this sample was highly compressible. The curing period while fabricating the samples did not play a major role in behavior of the wood composite, and this is seen when the 4%MDI140S, 4%CS4%MDI140S, and 4%CS4%MDI600S are compared. From the dynamic stress-strain relationship, it was observed that the stress-strain curve of the 4%MDIHP140S composted was clearly differentiated from the rest of stress-strain curves. This shows that the amount of pressure applied during the fabrication process had a large effect on the dynamic response of the wood. The "4%MDIHP140S" sample had a much greater stiffness value in comparison with the other samples. All of the samples were flexible in comparison with the "4%MDIHP140S" sample.

The results illustrate that the entire specimen has not been extensively damaged at the peak stress. It appears that compression failure is dominated by plastic deformation at peak load followed by debonding of the interface between constituents. In Figure 3.5a, stress-strain curves for 4%MDI HP140S are plotted for the three different strain rates. It can be observed that material behavior is dependent on the applied strain rate on to the specimen during the SHPB experiment. For 4%MDI HP 140 S, at a highest strain rate of 793 s^{-1}, the peak stress was

observed around 105 MPa, which is 25 psi higher than the peak stress observed at a lower strain rate of 600 s^{-1}. In Figure 3.5b, stress-strain curves for 2%CS2%MDI 140S are plotted for the three different strain rates. It can be observed that material behavior is independent of the applied strain rate on the specimen during the SHPB experiment. There was not much difference in the peak stress at the three different strain rates. It was observed that material yielded without much variation in the stress. The same materialistic behavior was observed in the other seven materials as observed in Figure 3.5b.

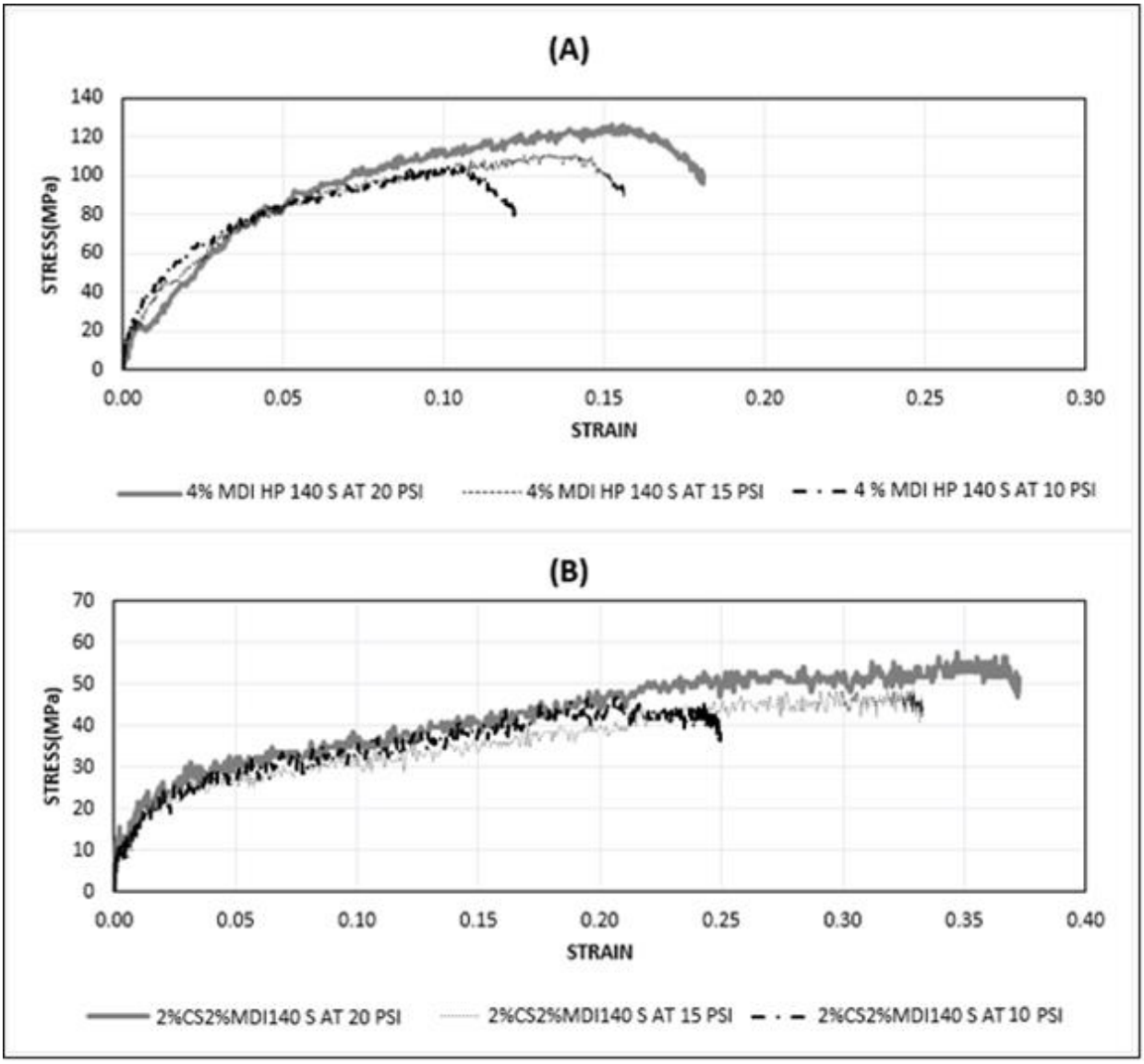

Figure 3.5- Effect of Strain Rate on wood based bio-composites: (A) Effect of Strain Rate on 4% MDI HP 140 S (B) Effect of Strain Rate on 2%CS2%MDI 140 S

Table 3.2 shows that the 4%MDI4%CS 600S sample had the highest average strain rate. This was followed by the 4%MDI1%MCC140S sample at all the three loading pressures. Samples containing CS had a high average strain rate when compared with other wood samples, and this shows that the CS contributed to the high stain rate of the material. The 4%MDIHP140S

sample had the lowest strain rate, and the 4%MDI140S sample consistently had a high strain rate.

Table 3.2: Average Strain Rate and Specific Energy at different strain rates

No.	TYPE of WOOD BASED BIO-COMPOSITE	Average strain at 10 psi (s^{-1})	Specific Energy at 10 psi (kJ/kg)	Average strain at 15 psi (s^{-1})	Specific Energy at 15 psi (kJ/kg)	Average strain at 20 psi (s^{-1})	Specific Energy at 20 psi (kJ/kg)
1	4%MDI HP 140 S	600 ± 30.9	10.6 ± 1.38	709.3 ± 19	13.1 ± 0.12	793 ± 56.9	17.2 ± 1.4
2	4%MDI, 4%CS 600S	1143.3 ± 92	15.1 ± 1.5	13545 ± 16.7	18.8 ± 0.2	1644.7 ± 68.9	26.6 ± 1.6
3	4%MDI140S	857.5 ± 4.9	11.01 ± 0.2	1113 ± 16.9	15.9 ± 0.3	1209.7 ± 11.5	20 ± 0.1
4	2%MDI, 4%CS 140S	943.5 ± 25.1	11.13 ± 0.34	1267 ± 6	15.3 ± 0.1	1454.5 ± 76.7	19.2 ± 0.4
5	2%MDI, 2%CS 140S	947 ± 25.8	11.9 ± 0.04	1236.25 ± 4.1	16.9 ± 0.2	1373.66 ± 15.5	21.7 ± 0.15
6	4%MDI, 4%CS 140S	930 ± 1.8	12.38 ± 0.35	1195.3 ± 32.2	16.5 ± 0.5	1335.7 ± 79.7	19.6 ± 1.8
7	4%MDI, 2%CS 140S	1055.3 ± 44.9	11.9 ± 0.3	1175 ± 9.1	18.9 ± 0.2	1546 ± 14	20.43 ± 0.7
8	4%MDI, 1%MCC 140 S	887 ± 8.5	11.01 ± 0.2	1143 ± 19.8	17.5 ± 0.5	1248.33 ± 16.6	22.08 ± 0.5
9	4%MDI, 2%MCC 140S	1063.75 ± 9.1	11..3 ± 0.2	1258.75 ± 21.7	16.2 ± 0.4	1571 ± 18.7	20.5 ± 0.15

This shows that compression pressure applied during the fabrication process of the wood composite plays a major role in enhancing these properties. The specific energy for the 4%MDI4%CS 600S sample was the highest among all the samples. The samples containing CS also had an important role in the specific energy of the material. The lowest specific energy was

found from the control sample, 4%MDIHP140S, and this again proves that how highly elastic this material is.

3.5 Conclusion

Nine wood-based bio-composites were studied for high-stain rate compressive loading using the SHPB test. It was found that the composite created at the highest pressure (4%MDIHP140S) had the greatest stiffness among all the samples. This shows that improved composite stiffness can be achieved when material is compressed at a higher pressure during the fabrication process. The sample containing a solid content of 4% MDI and 4% CS pressed at 600 s had the highest average strain rate and specific energy. The samples containing CS showed enhanced properties, and therefore CS can be a good constituent for making wood-based bio-composites. The applications of these samples can be various including being used as packaging material where they can sustain dynamic impact.

3.6 Future Scope

DIC analysis can be done on all the wood samples. The following wood samples can be studied under blast loading.

CHAPTER IV

STUDY OF VARIATION IN NATURAL FREQUENCIES OF BIO-COMPOSITES DUE TO STRUCTURAL DAMAGE

4.1 Introduction

Every structure and machine has a natural frequency. If machines and structures are designed correctly, these natural frequencies will not affect the operation or reliability of the machines. The role of composite materials increases continuously because of their high mechanical characteristics to weight ratio. Extensive research has been done in the area of bio-composites because this area has many advantages including the low manufacturing costs involved in producing final products and producing highly valued products from low-value materials. Producing biodegradable products has become a necessity due to petroleum-based products being a finite resource and having more potential to harm the environment. Shah et al [40] studied behavior of nine different bio-composites under compressive loading and found how different constituents used in producing a bio-composite can change the dynamic behavior of the material. Many researchers have detected shifts in the natural frequency when there was damage in the structure or material. I Negru et al [41] studied how transverse cracks in structures affect their stiffness as well as natural frequency. Ján Svoreň et al [42] studied how the natural frequencies of the circular blade can be obtained through various methods. Rangel et al [43] analyzed the shift in natural frequencies of structures and proposed the best method to repair damaged bridges. Magara et al [44] proposed a theoretical method to find the natural frequency for centrifugal pumps which were verified with experimental methods. Their results indicated

that for high density centrifugal compressors, some natural frequencies of an impeller increased with a high-density gas.

The modal analysis ensures the likelihood of global approval for a whole structure. Initially experimental modal analysis was carried out using a cantilever beam vibration technique. Many composites have been studied for their vibrational behavior [45-47]. To gauge the mechanical properties and physical properties of wood and wood-based composites, vibrational methods have been successfully used for many decades in forest product industry and scientific research [48-50]. Previously, natural frequency and the dynamic modulus of elasticity have been found using vibration beam technique. Zeng Wany et al [51] obtained the dynamic modulus of elasticity and damping ratio the through same technique and compared them for three commercially available wood- based composites.

Finite element analysis (FEA) has been previously used to compute M and K matrices to determine the mode shape and natural frequencies. ABAQUS is a commercially available FEA code that has been used by many researchers to compute such parameters. Bimal Bastin et al [52] used ABAQUS to obtain the static displacement and principle stress of a wheel rim. Zhou Kaihong[53] studied modal analysis in ABAQUS on an oval gear. K. Kharate et al [54] predicted squeal and studied natural frequency, and mode shape of a rotor brake using experimental modal analysis and finite element analysis. They concluded that the material properties of a brake disk play an important role in determining vibration mode patterns W. R.Taylor et al [55] determined the elastic constants of an orthotropic bone using FEA and Modal Analysis.

Various studies have been carried out to predict a shift in natural frequency, change in stiffness due to damage, and other varying parameters like density of the structure using various

methods. This study precisely uses experimental modal analysis to predict a shift in the natural frequency of the material due to damage and compare the shift that of the SYP-SP bio-composite with a commercial SYP composite.

4.2 Materials

Specimens were created from primarily southern yellow pine (SYP) (2-3 mm particle size), 4 wt% (solids basis) sweet potato (SP) particles (~1 mm particle size), and 4 wt% (solids basis) methylene diphenyl diisocyanate (MDI) resin. MDI is an aromatic diisocyanate and was an efficient binder that has been used within the production of composite wood products for over 30 years. The SYP was mixed in a rolling mixer as MDI resin was sprayed into the mixer with a paint sprayer. Before spraying the MDI, precautions were taken by using PPE which covered the researcher, including a full face mask with a P-100 activated carbon filter which was discarded after 4 hours of being opened from the original package and a new filter was used after that point. The amount of mass used to create the panels was the same for each panel (approximately 2.95 kg). The 22” x 24” panels were manufactured by using a mold and half of the SYP/MDI was put into the mold and leveled to form a level layer. Next the SP particles were shaken onto the top of the layer, and then the remaining SYP/MDI was input into the mold. The material was leveled and pressed with approximately 50 lbf to produce a mat. Next, the mat was put on two steel platens that were sprayed with a silicone based release agent. A Dieffenbacher 915 mm x 915 mm hot press system located at the Sustainable Bioproducts Laboratory at Mississippi State University was used to create the panels used in this study. This hot press with steam injection capability was coupled with the Alberta Research Council's Pressman operation and monitoring software. The parameters used to form the 22” x 24” panels included a temperature of approximately 185^{o}C, a mat pressure of approximately 8.5 MPa and a total moisture content of 6

wt%. The Dieffenbacher hot press formed the panel based on the desired thickness of 0.25 inches. The pressure required to form the panel to the appropriate thickness was based on the ability of the composite material in the mat to be compressed to the appropriate thickness. Is the resin fully sealed pores in the wood?

Resin does not fully sealed pores in the wood; p-MDI's isocyanate groups can react with hydroxyl groups in wood and moisture to form irreversible urethane linkages. p-MDI penetrates into the amorphous regions of the wood furnish cell walls, interweaving on the molecular level until it "plasticizes" the wood cell wall itself . p-MDI's thermosetting linkage is irreversible, giving the board a degree of moisture resistance. These helps to make the MDI-bonded boards perform better when exposed to moisture.

4.3 Specimen Preparation

Specimens of both the commercial SYP composite and the SYP-SP based bio-composite were prepared. The specimens measured 226.7mm x 25.8 mm x 6.64 mm. The specimen that was damaged had the damage induced from a distance of two inch from the fixed end and the damage was hole of 0.5" diameter.

4.4 Experimental Procedure and Setup

The natural frequencies of damaged and undamaged commercially available SYP and the laboratory produced SYP-SP bio-composite were obtained through experimental modal analysis (cantilever beam vibration technique), and the modulus of elasticity in flexural mode was obtained from it. Separate tests were carried out to get the Poisson's ratio of the material. All these parameters were imported into FEA software and natural frequencies for both cases (damaged and undamaged) were obtained and thus verified.

Frequencies for the damaged and undamaged specimens were obtained through vibration beam technique. The setup is situated in the structure and dynamics lab of University of Mississippi. The figure below shows the schematic of the setup.

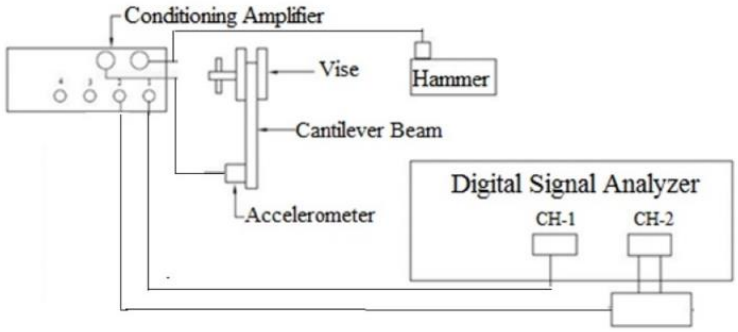

Figure 4.1: Schematic of cantilever beam vibration technique through hammer excitation

An impact hammer was used to excite the beam. The accelerometer detected the response of the beam. Time-dependent responses from the impact hammer and accelerometer were amplified through power amplifiers and then converted into Frequency Response Function (FRF) in the Dynamic signal analyzer (Hewlett Packard, Model #35665A). This analyzer displayed the imaginary component of the FRF magnitude. The peak amplitudes of this display were plotted accordingly to determine three different mode shapes of the beam at three respective natural frequencies.

The Poisson's ratio of the material was found in accordance with the ASTM standard E132–04 [56]. Poisson's ratio of the two materials was found by testing the materials in tension in a material testing system (MTS) machine (model LVDT, serial number 10252898) situated in the structures and dynamic laboratory of the University of Mississippi. Tension was applied in the longitudinal direction of the specimen. An extensometer (model 354-025M-025-ST) which

had a gauge length of 25mm, was used to measure the strain in the longitudinal and transverse direction of the material.

Initiating finite element analysis in ABAQUS, the cantilever beam was drawn to the specifications outlined in the material section and other properties were taken from the two experiments mentioned above. After applying the material properties, the following issues were addressed: boundary conditions, mesh resolution, and mesh refinement. When modeling the cantilever beam, the first assumption was that the beam was fixed in an encastre condition to replicate the experimental conditions. Using this assumption, the necessary boundary conditions were met. To validate the ideal 1D conditions, an in-plane boundary condition was applied. However, the in-plane boundary condition constrained the beam and yielded no results. After yielding no results, the decision to use only use the encastre condition was made.

After the boundary conditions are dtermined, a mesh is applied. Initially, a default mesh was used and the simulation poorly depicted the experimental results. The coarse mesh yielded uneven displacement contours and an incorrect visual representation of the problem. In the cantilever beam application, a coarse mesh caused poor resolution and artifacts in the FEA software. This error led to the decision to further increase the mesh size. After the mesh size was increased, the displacement contours improved substantially.

4.5 Experimental Results and Analysis

The dynamic modulus of elasticity in flexure was obtained from the cantilever vibration beam technique. They were $E_{undamaged}$ =2.25 GPa and $E_{damaged}$=2.24 Gpa for the commercial SYP composite. The SYP-SP composite had a modulus of $E_{undamaged}$ =3.04 GPa and $E_{damaged}$=3.02 GPa

for the undamaged and damaged sample, respectively. Densities for undamaged and damaged specimens are shown in Table 4.1.

Table 4.1: Densities of Materials before and after Damage.

Material	Undamaged	Damaged
SP-Wood	910.724 kg/m^3	906.33 kg/m^3
Commercial Wood	773.273 kg/m^3	768.7 kg/m^3

Table 4.1 shows that the density of each material decreased with the induction of damage. The density of SYP-SP composite was much higher than the commercial SYP composite such that there was more fiber concentration in the material.

Figure 2 shows three mode shapes obtained through the cantilever beam vibration technique, and these mode shapes show how the material vibrated at resonance. Resonant vibration is mainly caused by an interaction between the inertial and elastic properties of the materials within a structure. The displacement of the SYP commercial composite for mode one was almost constant, while the SYP-SP composite varied. When these materials were excited and their excitation matched their first natural frequency, this vibration pattern occurred.

The displacement profile for the second mode was almost the same for both materials, while the third mode displacement coutour for the SYP-SP composite was not as smooth as the SYP commercial composite, but there were node points at similar locations.

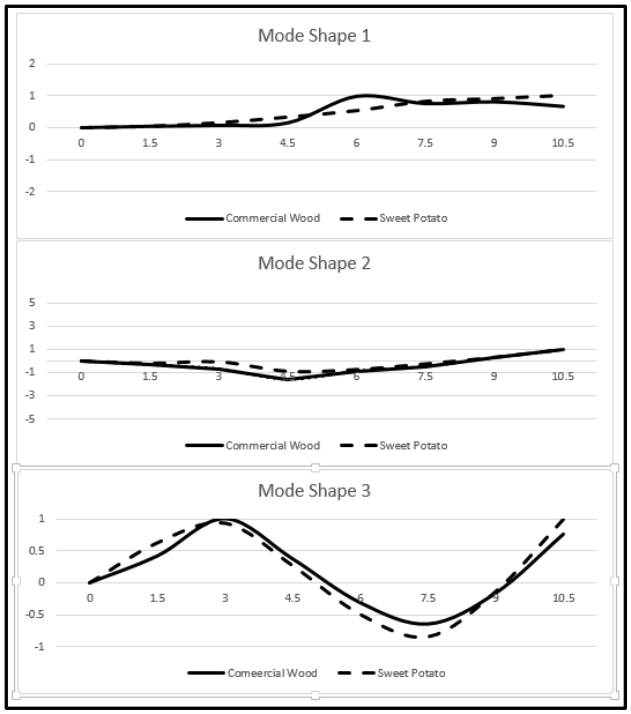

Figure 4.2: Mode shape comparison of commercial wood and SP-wood obtained through cantilever beam vibration technique

The Poisson's ratio of the materials was $\mu_{SP-Wood} = 0.104$, $\mu_{Commercial\ Wood} = 0.04$. All these parameters were imported into ABAQUS and natural frequencies for both damaged and undamaged cases were obtained

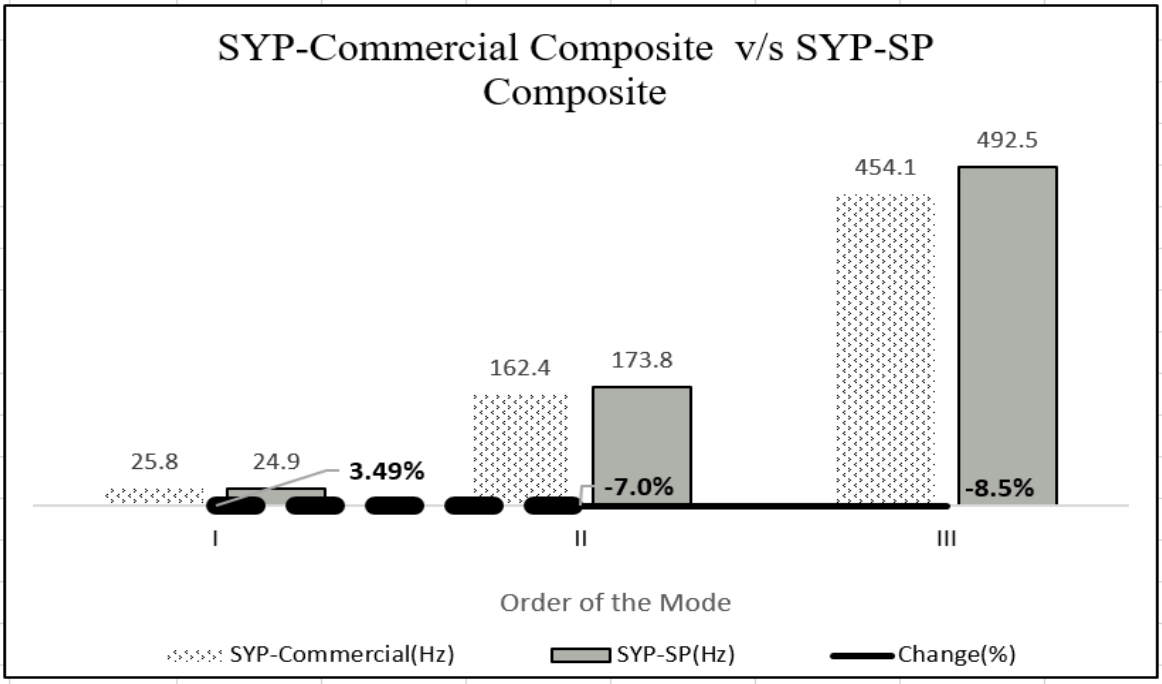

Figure 4.3: Comparison of natural frequency of undamaged materials

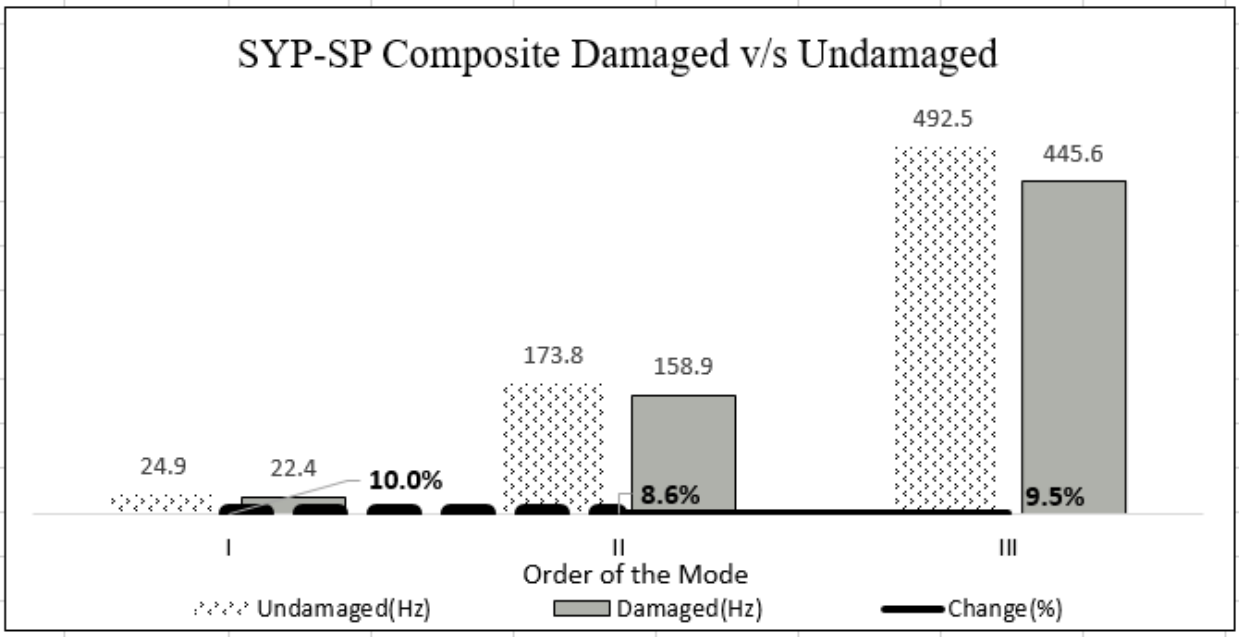

Figure 4.4: Comparison of natural frequency of damaged and undamaged SP-wood.

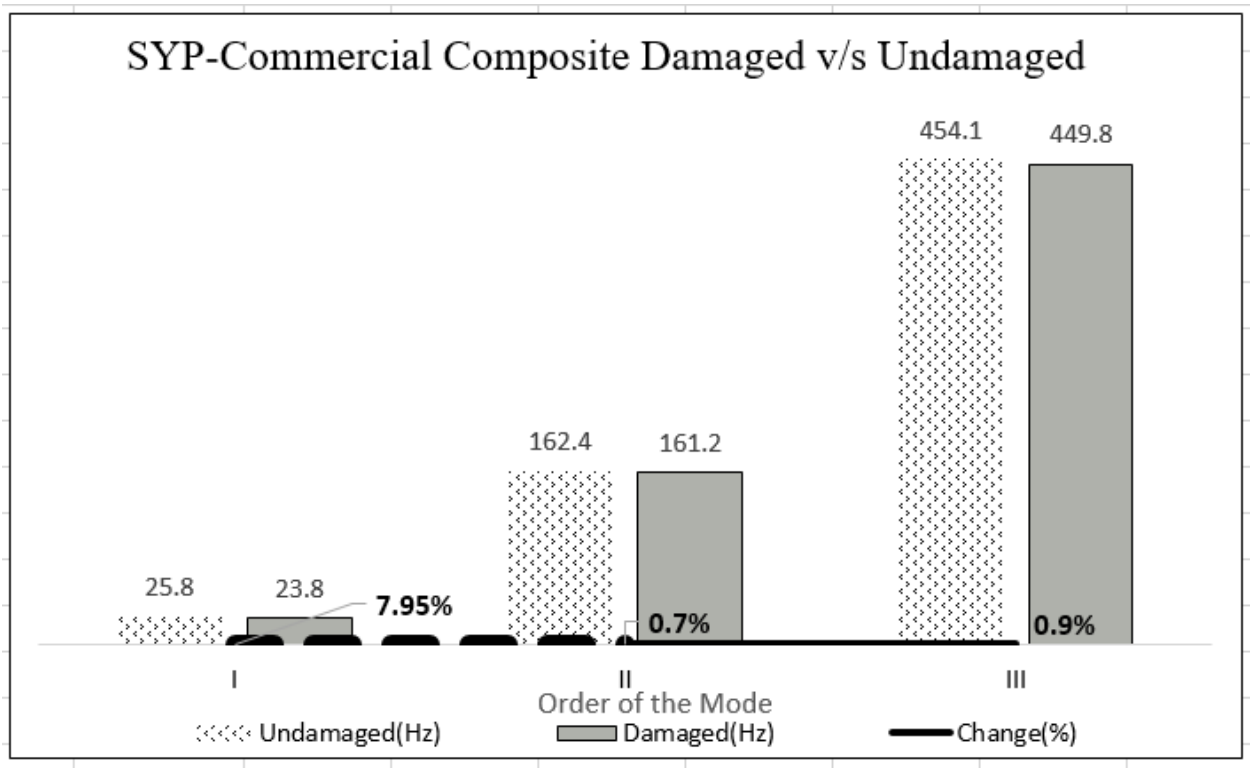

Figure 4.5: Comparison of natural frequency of damaged and undamaged commercial wood.

Figure 4.3 shows that the natural frequencies of the SYP commercial composite increased as the order of the mode increased in comparison to the SYP-SP composite, although their initial frequencies were similar. This also shows that the variation in natural frequencies was seen more in the commercial composite rather than in the SYP-SP composite.

The SYP-SP composite showed more sensitivity towards damage in comparison to the SYP commercial composite when comparing the damaged v/s undamaged results shown in Figure 4.4, and 4.5. The first three natural frequencies obtained for the SYP-SP composite were 24.925 Hz, 173.75 Hz and 492.5 Hz, respectively. After damage was induced, a change of 10%, 8.6%, and 9.5% was realized, respectively. As far as the commercial SYP composite was

concerned, the first three natural frequencies obtained were 25.75 Hz, 162.38 Hz and 454.12 Hz, respectively. When damage was induced there was a change of 7.95%, 0.7%, and 0.9% respectively. The change was obtained by equation 1, where $f_{UNDMAGED}$ is the experimental frequency of undamaged material and $f_{DAMAGED}$is the frequency of damaged materials. This shows that the commercial SYP composite had more sensitivity towards damage.

$$\Delta f(\%) = \left(\frac{f_{UNDMAGED} - f_{DAMAGED}}{f_{DAMAGED}}\right) * 100 \qquad (1)$$

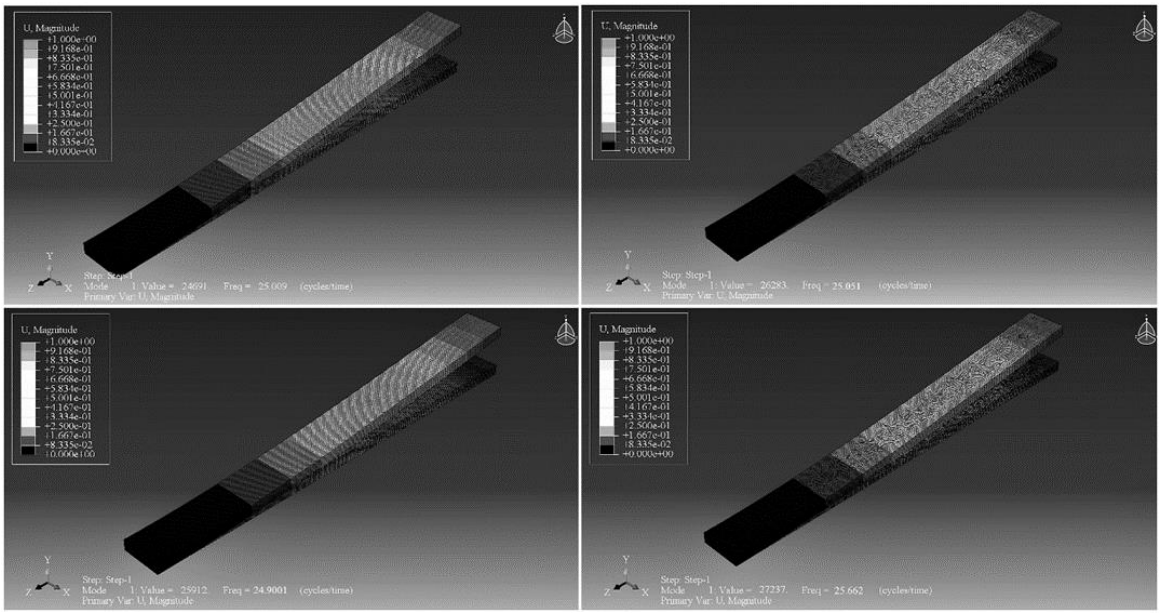

Figure 4.6: FEA Analysis

Table 4.2: Comparison of experimental data with FEA data

Bio-composites	Undamaged			Damaged		
	Experimental Frequency (Hz)	*FEA* Frequency (Hz)	Error (%)	Experimental Frequency (Hz)	*FEA* Frequenc y (Hz)	Error (%)
SYP-SP Composite	24.9	25.0	-0.3	22.4	22.4	-0.2
	173.8	171.5	1.3	158.9	157.0	1.2
	492.5	485.5	1.4	445.6	438.0	1.7
Commercial SYP Composite	25.8	24.9	3.3	23.75	23.2	2.2
	162.4	155.9	4	161.2	153.8	4.6
	454.1	434.9	4.2	449.8	422.4	6.1

The results here clearly depict a frequency change which shows that damage in the material is affecting its performance. Table 4.2 shows agreement between the experimental data and the FEA predictions. A maximum frequency error of 6% was found over the first three mode shapes. The error was calculated using the equation 2 below:

$$Error(\%) = \left(\frac{f_{EXP} - f_{FEA}}{f_{EXP}}\right) * 100 \quad (2)$$

f_{EXP} is the experimental frequency found while performing the experiment, and f_{FEA} is the frequency found after running the FEA simulation. The variation in the results between the FEA predictions and Experimental data may be because when slight damage occurred, the domain signal from the dynamic signal was discrete, as there were intervals among the spectrum lines so that the change of the natural frequency could not be reflected in FRF. The damaged sample's signal could have been submerged by the error caused by the spectrum interval; therefore, when the variation of the natural frequency was small, the damage calculated deviated much more from the practical condition

4.6 Conclusion:

This study compared the material behavior between a commercially available southern yellow pine (SYP) particle board composite and a SYP-SP (sweet potato) composite when damage was induced in them using the parameter of natural frequency. Based on above results and discussion it can be stated that the commercial SYP-SP composite showed more sensitivity towards damage in comparison to the SYP commercial composite. The natural frequencies of SYP-SP did not vary as much as SYP commercial composite when the order of the mode increased. When damage was induced in the SYP-SP composite, the shift for first three natural frequencies were 10%, 8.6%, and 9.5%and for SYP-Comericial composite was 7.95%, 0.7%, and 0.9% respectively

CHAPTER V

DETERMINATION OF POISSON'S RATIO, DYNAMIC MODULUS OF ELASITICTY AND YOUNGS MODULUS OF WOOD-BASED BIO-COMPOSITES.

5.1 Introduction

This study compares the behavior of wood-based bio-composite on the basis of the Poisson's ratio by conducting longitudinal tension tests on small tests specimens and compares young's modulus to that of dynamic modulus of elasticity based on flexural vibration (MOE_F). Three replicates of each type of bio-composite were tested, so as to get accurate results. Knowledge of mechanical properties is necessary, especially large-span structures, such as bridge structures. Poisson's ratio of wood made up of sweet potato flour was highest among all the bio-composites whereas the Poisson's ratio of wood made up off pure cotton was the lowest. The maximum variation between Young's modulus to that of MOE_F was found in Cotton Motes MCC with 28.12% increase and lowest was found to be in pure cotton-wood with increase of 24%.

Research on green composites has become one of the major areas of interest in recent times. The importance of research in this area has increased mainly because of the high performance in mechanical properties, many processing advantages, low cost and lightweight,

availability and renewable, cheap, environmentally friendly, degradability and recyclability properties [58]

Properties of materials like strength, elastic constants, and other material properties as well as their performance under a variety of actual conditions and environments are required. They are necessary because they are used for two primary purposes: Engineering design (for example, failure theories based on strength, or deflections based on elastic constants and component geometry) and quality control either by the materials producer to verify the process or by the end user to confirm the material specifications. Poisson's ratio is one of the most important material property. In comparing a material's resistance to distort under mechanical load rather than to alter in volume, Poisson's ratio offers the fundamental metric by which to compare the performance of any material when strained elastically. Convoluting mechanical response at the atomic level with the intervening linkages to the macroscopic scale, Poisson's ratio provides a universal way to contrast the structural performance of real materials, whether homogeneous or not.

Materials with different Poisson's ratios behave very different mechanically. Properties range from 'rubbery' to 'dilatational', between which are 'stiff' materials like metals and minerals, 'compliant' materials like polymers and 'spongy' materials like foams. The physical significance of ν is revealed by various interrelations between theoretical elastic properties.[59]

Thomas, found Poisson's ratio of oriented strand board. In the study, the experimentally determined Poisson's ratio appears consistent with the values estimated from the panel shear and

tension moduli of elasticity [60]. Mascia et al examined the numerical variation of Poisson's ratio with fiber direction for the tropical wood species Goupia glabra, whose products have significant applications in civil construction [61]. Gercek, examined the values and applications of Poisson's ratio in rock mechanics. In the study, the effects of Poisson's ratio in the elastic deformation of materials, intact rocks, and rock masses are briefly reviewed [62].

Mizutani et al, this study investigates the effect of a wide range of moisture contents (0 - 177 %) on the Poisson's ratio of wood taken from Japanese cypress and magnolia by conducting longitudinal compression tests. The study states that when the moisture content is below the respective fiber saturation point Poisson's ratio decreases with increasing moisture content. In contrast, at moisture contents above the fiber saturation point, the Poisson's ratio increases with moisture content. In the study, the same tendency was observed in both wood species, but the effect was more pronounced in magnolia than Japanese cypress [63].

The Poisson's effect of three bio-composites namely cotton motes MCC, Pure cotton, Sweet Potato and commercial wood have been investigated and compared to give insight into the mechanical properties of these materials which can further be used in various designs which involve these new bio-composites.

5.2 Material

The material investigated in this study involved different types of wood-based bio-composites created with waste cotton motes (cotton gin trash), pure cotton, and sweet potato flour. Cotton, in its natural state is a difficult material to mix homogeneously with wood. Both

the cotton motes and pure cotton were processed into a fine powder by using a large heated vat and motorized agitator with muriatic acid (HCl). An amount of 7.27 liters of water and 1.82 liters of muriatic acid (31.45% weight HCl) was mixed with about 380 grams of cotton or cotton motes to create the powder at a temperature of 80^{o}C for 1 h. The majority of each composite was created using ~2.5-3.0 mm southern yellow pine particles that had been hammer milled. The particles were input into a forming box (measuring 559 mm x 610 mm) using a composition of 92% southern yellow pine particles, 4% methylene diphenyl diisocyanate (MDI), and 4% additive (cotton motes, pure cotton, or sweet potato flour) on a solids basis. A moisture level of 6% was used as the starting moisture for the additive and wood mixture before the MDI was added in the rolling mixer using a pneumatic sprayer. A Dieffenbacher 915 mm x 915 mm hot press system located at the Sustainable Bioproducts Laboratory at Mississippi State University was used to create the panels used in this study. This hot press with steam injection capability was coupled with the Alberta Research Council's Pressman operation and monitoring software. The Dieffenbacher hot press forms panels based on the desired thickness, so each composite material had differing pressures which were required to produce a panel with a thickness of 6.35 mm. The varying pressure required to form the panel to the appropriate thickness was based on the ability of the composite material in the mat to be compressed to the appropriate thickness. Although the starting mass for each panel was similar, the Dieffenbacher press controlled the pressure to form a panel with a particular thickness. The cotton motes additive panel was formed at a pressure of 8.5 MPa and density of 675 kg/m^3, the pure cotton additive panel was formed at a pressure of 6.2MPa and density of 710 kg/m^3, and the sweet potato flour additive panel was formed at a pressure of 8.5 MPa and density of 710 kg/m^3.

5.2 Experimental procedure and results

The Poisson's ratio of the material was found in accordance with ASTM standard -- E 132 – 04 Poisson's ratio of the two materials were found by testing the materials in Tension in MTS machine (Model# LVDT, Serial number 10252898). The tension was applied in the longitudinal direction of the specimen. Extensometer (Mode# 632.85E-14) which had a gauge length of 1 inch in axial and longitudinal direction, was used to measure strain in the longitudinal and transverse direction of the material.

The specimen was adjusted on to the MTS testing machine. Load was applied on the the specimen in tension until the specimen fractured, the readings were transported to softhware called station manager.

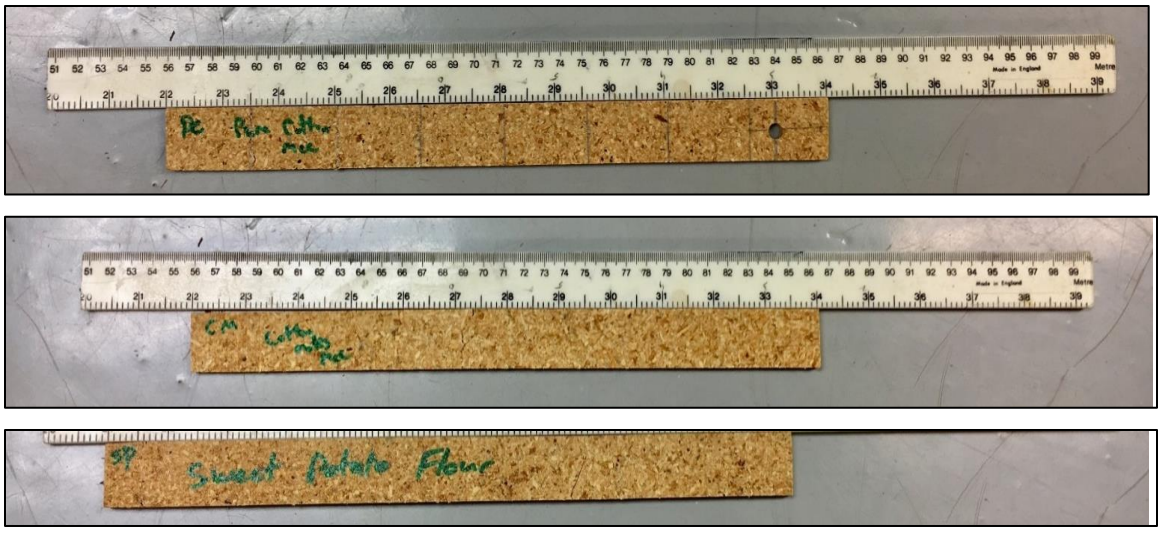

Figure 5. 1: Samples of bio-composities

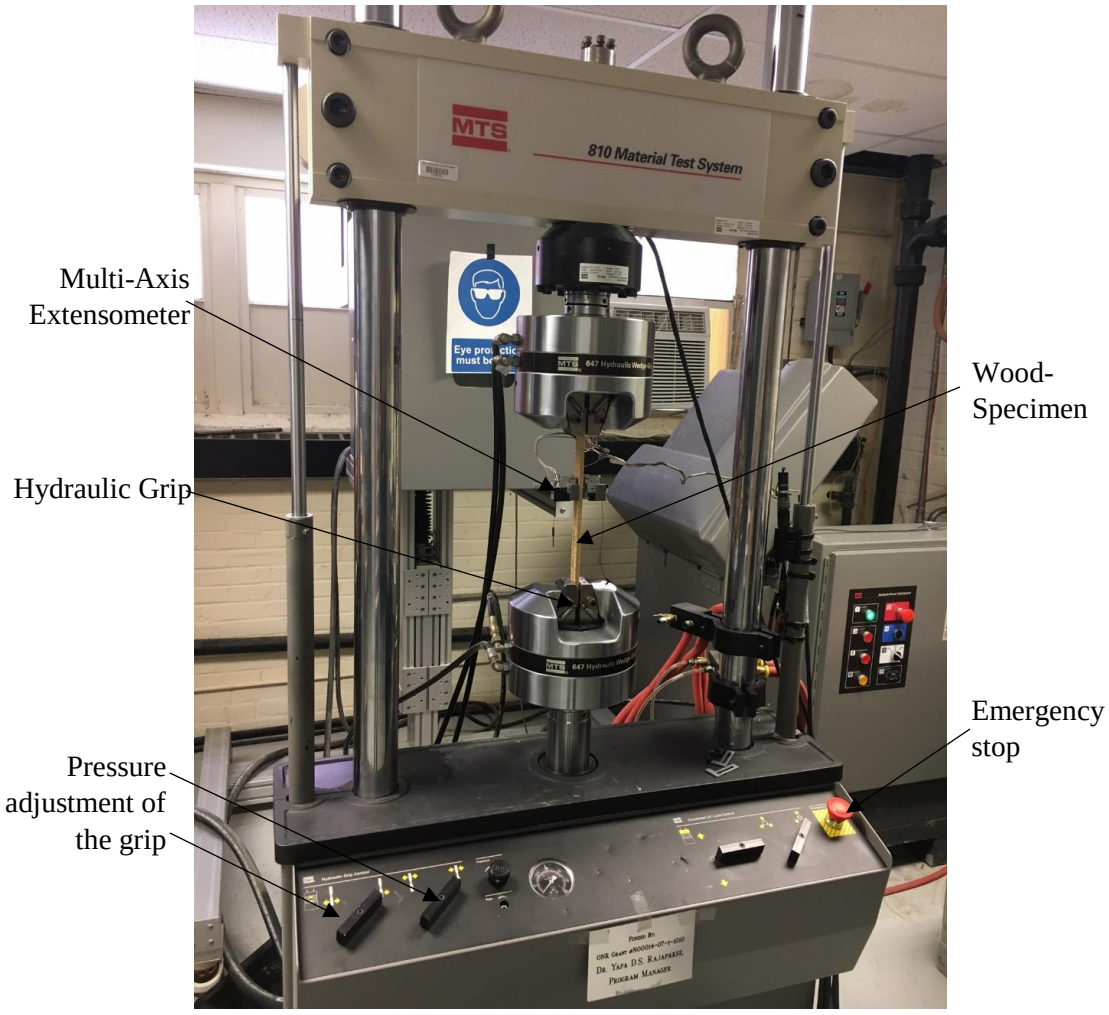

Figure 5 2: Experimental setup

For obtaining the Young's modulus of the specimens the load applied by the incremental load by MTS machine was multiplied with the cross section of the specimen which is 1.02in x 0.26in, thus the results obtained were in lbf/in^2 which were converted in Gpa by the relation of 1 lbf/in^2 = 0.000006895 Gpa. Thus the Young's Modulus was obtained.

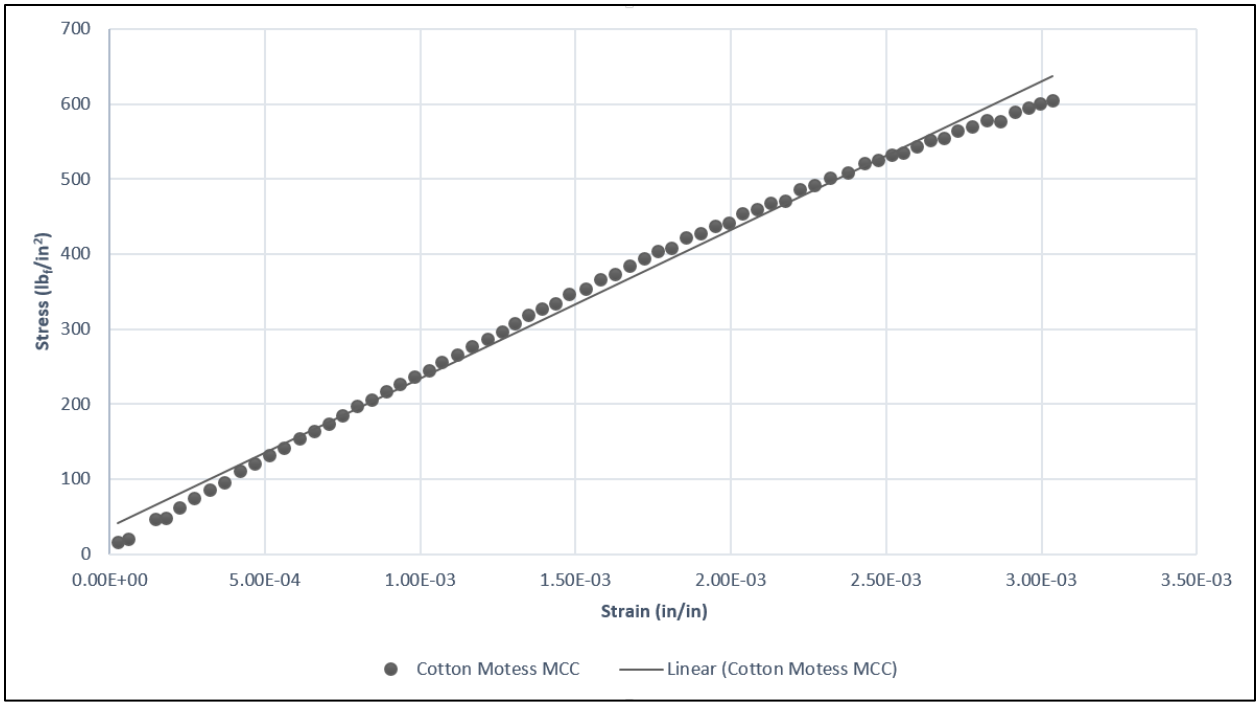

Figure 5.3 Sample Stress-Strain cure for Cotton Motes MCC

Table 5.1: Poisson's Ratio of bio-composites

Materials	Mean Value of the Poisson's ratio	No of observations	Standard deviation	Error
cotton motes	**0.344**	3	0.038	**±0.022**
pure cotton	**0.167**	3	0.034	**±0.019**
sweet potato	**0.363**	3	0.019	**±0.028**

The above figure describes that the Poisson's ratio of sweet potato is the highest where as that of pure cotton is lowest. This shows that sweet potato wood is highly elastic as the ratio of its longitudinal deformation to transverse deformation is very less' where as the Poisson's ratio

of pure cotton shows that the material is rigid or it is highly stiff or it is less elastic in compare to all other materials mentioned in this study.

The Dynamic Modulus of Elasticity was taken from the previous study (Shah et al, 2017). Both young's modulus are compared and shown below. The maximum variation between Young's modulus to that of MOE_F was found in Cotton Motes MCC with 98.48% increase and lowest was found to be in Commercial wood with increase of 94.42%. It shows that while designing, the loading condition of the object is of utmost necessity as there is huge variation in Young's Modulus and MOE_F. The increase in all the materials can be stated as almost similar as seen in the graph below, the slope of the line is seen to be very less

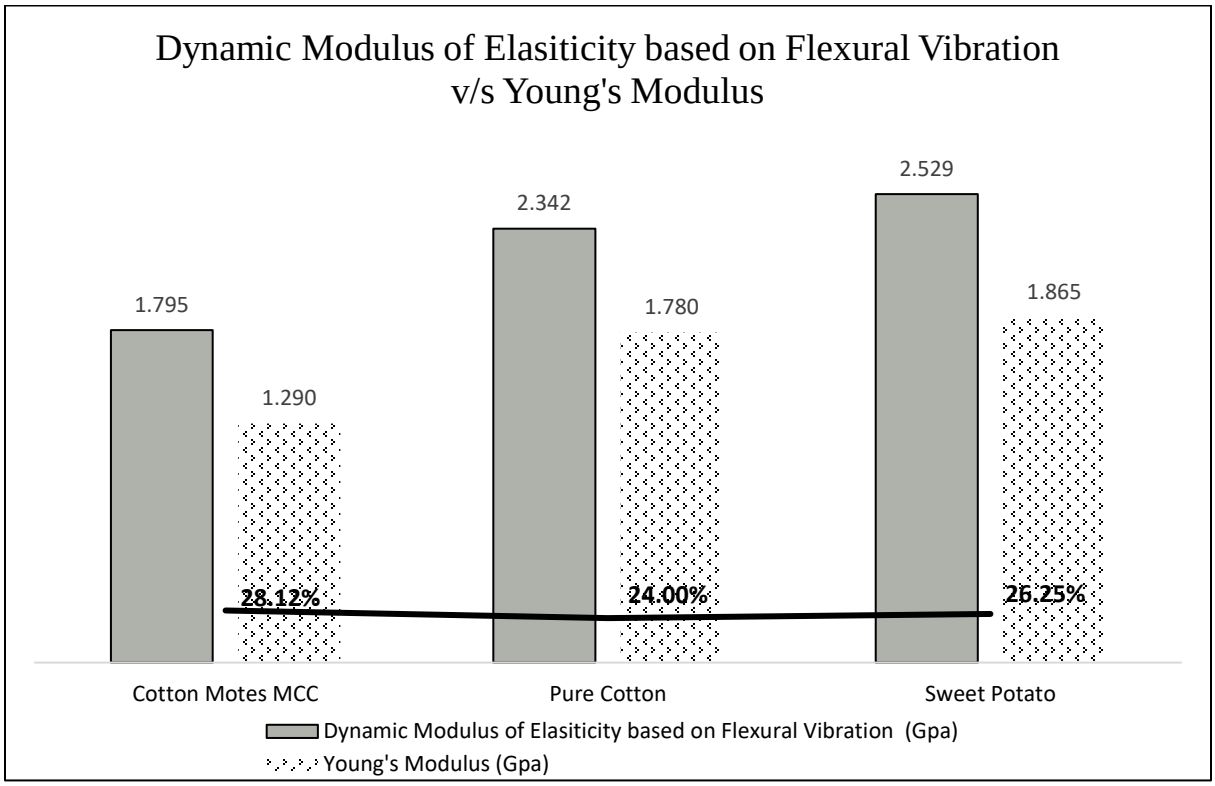

Figure 5.4: Dynamic Modulus of Elasticity based on Flexural Vibration v/s Young's Modulus

The above results are in accordance with Hasan et al. [65] where they found the variance between the static and dynamic Young's Modulus of Scot pine and the maximum variance was 30.1%.

VI. CONCLUSION

In all thirteen bio-composites were prepared and were analyzed for their dynamic characteristics. In them, nine bio-composites were studied under three different high strain rates, and it was found that the composite created at the highest pressure (4%MDIHP140S) had the most significant stiffness among all the samples and Corn Starch could be a right constitute for making wood-based bio-composites was the conclusion. When damage was induced in the SYP-SP composite, the shift for first three natural frequencies were -0.075%, 0.6%, and 1.2% respectively the shift for the SYP commercial composite were -0.5%, -5.12%, and -19% respectively. Poisson's ratio of three bio-composites made out of cotton motes, pure cotton, sweet potato was experimentally founded to be 0.344, 0.167, 0.363 respectively. Comparison between the Young's Modulus and dynamic modulus of elasticity based on flexural vibration (MOE_F) of these bio-composites was done and variation was found to be 28.1%, 24% and 26.3% respectively.

REFRENCES

[1] Ho, M.-P., Wang, H. and Lee, J.-H., Ho, C.-K., Lau, K.-T., Leng, J.S. and Hui, D. (2012) Critical Factors on Manufacturing Processes of Natural Fibre Composites. Composites: Part B, 43, 3549-3562. http://dx.doi.org/10.1016/j.compositesb.2011.10.001

[2] Sathishkumar, T.P., Navaneethakrishnan, P. and Shankar, S. (2012) Tensile and Flexural Properties of Snake Grass; Natural Fiber Reinforced Isophthallic Polyester Composites. Composites Science and Technology, 72, 1183-1190. http://dx.doi.org/10.1016/j.compscitech.2012.04.001

[3] Franco CR, Cyras VP, Busalmen JP, Ruseckaite RA, Vazquez A. Degradation of polycaprolactone/starch blends and composites with sisal fibre. Polym Degrad Stab 2004;86:95e103.

[4] Kim MN, Lee AR, Yoon SJ, Chin IJ. Biodegradation of poly(3- hydroxybutyrate), Sky-Green and Mater-Bi by fungi isolated from soils. Eur Polym J 2000;36:1677e85.

[5] Okada M. Chemical syntheses of biodegradable polymers. Prog Polym Sci 2002;27:87e133.

[6] Mohanty AK, Misra M, Hinrichsen G. Biofibre, biodegradable polymer and bio-composites.MacromolMater Eng 2000;266/277: 1e24.

[7] Wu CS. Physical properties and biodegradability of maleated polycaprolactone/starch composite. Polym Degrad Stab 2003;80: 127e34.

[8] Plant/Crop-based Renewable Resources 2020, URL: http://

[9] The Technology Roadmap for Plant/Crop-based Renewable

[10] A. K. Mohanty, M. Misra, and G. Hinrichsen (2000) Macromol.

[11] A. K. Mohanty, M. Misra, and L. T. Drzal (2001) Compos. Interf.

[12] A. Scott (2000) Chem. Week. Sept. 13, 73

[13] Faruk, O., Bledzki, K.A., Fink, H-P., Sain, M. 2012. Bio-composites reinforced with natural rubber: 2000-

2010. Progress in Polymer Science reviews. 37:1552-1569.

[14] Girones, J., Lopez, J.P., Mutje, P., Carvalho, A.J.F., Curvelo, A.A.S., Vilaseca, F. 2012. Natural fiberreinforced thermoplastic starch composites obtained by melt processing. Composites Science and

[15] Kabir, M.M., Wang, H., Lau, K.T., Cardona, F. 2012. Chemical treatment on plant-based natural fiber reinforced polymer composites. Composites: Part B Overviews. 43:2883-2892.

[16] Zhang, M.Q., Rong, M.Z., Lu, X. 2005. Fully biodegradable natural fiber composites from renewable resources: All-plant fiber composites. Composites Science and Technology Journal. 65:2514-2525.

[17] Chong, E.L., Ahmad, I., Dahlan, M.H., Abdullah, I. 2010. Reinforcement of natural rubber/ high density polyethylene blends with electron beam irradiated liquid natural rubber- coated rice husk. Radiation Physics and Chemistry Journal. 79:906-911.

[18] Hybrid bio-composite from talc, wood fiber and bioplastic: Fabrication and characterization Sanjeev Singh , Amar K. Mohanty , Manju Misra
doi:10.1016/j.compositesa.2009.10.022

[19] Joshi SV, Drzal LT, Mohanty AK, Arora S. Are natural fiber composites environmentally superior to glass fiber reinforced composites? Compos Part AAppl

Sci Manuf 2004;35:371e6.

[20] Jawaid M, Khalil H, Hassan A, Dungani R, Hadiyane A. Effect of jute fibre loading on tensile and dynamic mechanical properties of oil palm epoxy composites. Compos Part B-Eng 2013;45:619e24.

[21] Koronis G, Silva A, Fontul M. Green composites: a review of adequate materials for automotive applications. Compos Part B-Eng 2013;44:120e7.

[22] O'Donnell A, Dweib MA, Wool RP. Natural fiber composites with plant oilbased resin. Compos Sci Technol 2004;64:1135e45.

[23] Ramesh M, Palanikumar K, Reddy KH. Mechanical property evaluation of sisal-jute-glass fiber reinforced polyester composites. Compos Part B-Eng 2013;48:1e9.

[24] Boopalan M, Niranjanaa M, Umapathy MJ. Study on the mechanical properties and thermal properties of jute and banana fiber reinforced epoxy hybrid composites. Compos Part B-Eng 2013;51:54e7.

[25] Da Silva F, Filho RDT, Filho JdAM, Fairbairn EdMR. Physical and mechanical properties of durable sisal fiberecement composites. Constr Build Mater 2010;24:777e85.

[26]. Azwa, Z.N., Yousif, B.F., Manalo, A.C., Karunasena, W. 2013. A review on degradability of polymeric composites based on natural fibers. Material and Design Reviews. 47:424-442.

[27]. Girones, J., Lopez, J.P., Mutje, P., Carvalho, A.J.F., Curvelo, A.A.S., Vilaseca, F. 2012. Natural fiberreinforced thermoplastic starch composites obtained by melt processing. Composites Science and Technology Journals. 72:858-863

[28] BergeretAnne, Environmental-Friendly Biodegradable Polymers and Composites. IntegratedWasteManagement, ed. by Sunil Kumar (InTech, 2011).

[29] A. Arbelaiz, B. Fernandez, A. Valea and I.Mondragon // *Carbohydrate Polymers* **64** (2006) 224

[30] Kawahara Y, Shioya M. Characterization of microvoids in Mulberry and Tussah silk fibers using stannic acid treatment. J Appl Polym Sci 1999;73:363–7.

[31] Afrough M, Pandya TS, Daryadel SS, Mantena PR (2015) Dynamic response of pultruded glass-graphite/epoxy hybrid composites subjected to transverse high strain-rate compression loading. Sci Res 6:953-962. http://www.scirp.org/journal/PaperInformation.aspx?paperID=61163

[32] Allazadeh MR, Wosu SN (2011) High strain rate compressive tests on wood. Strain 48:101-107. http://onlinelibrary.wiley.com/doi/10.1111/j.1475-1305.2010.00802.x/abstract

[33] Soheil Daryadel, Damian L. Stoddard, Arunachalam M. Rajendran(2014) Dynamic response of glass under high-strain rate compression loading. http://www.uab.edu/engineering/home/images/downloads/UAB_-_ECTC_2014_PROCEEDINGS_-_Section_2.pdf

[34] Bragov A, Lomunov AK (1997) Dynamic properties of some wood species. J Phys IV France 7:C3487-C3492. https://hal.archives-ouvertes.fr/jpa-00255541/document

[35] Dahal RP, Munn IA, Henderson JE (2013) Forestry in Mississippi: The impact of the industry on the Mississippi economy: An input-output analysis. Forest and Wildlife Research Center, Research Bulletin FO 438, Mississippi State University. 22 pp. http://www.fwrc.msstate.edu/pubs/forestryinmississippi_2010.pdf.

[36] Kolsky H (1949) “An Investigation of the Mechanical Properties of Materials at very High Rates of Loading “Proc Phys Soc B 62:676-699. http://iopscience.iop.org/article/10.1088/0370-1301/62/11/302/pdf.

[37] Weinong WC, Bo S (2011) Split Hopkinson (Kolsky) bar. DOI: 10.1007/978-1-4419-7982-7. ISBN 9781441979810 Springer

[38] Ramesh KT High strain rate and impact experiments *in* Handbook of experimental solid mechanics. Springer. Springer Handbook of Experimental Solid Mechanics. pp 929-960. 10.1007/978-0-387-30877-7_33

[39] Chauhan, Y.P., Sapkal, R., Sapkal, V., and Zamre, G. (2009). Microcrystalline cellulose from cotton rags (waste from garment and hosiery industries). Int J Chem Sci. 7(2): 681-688.(http://www.tsijournals.com/chemical-sciences/microcrystalline-cellulose-from-cotton-rags-waste-from-garment-and-hosiery-industries.pdf)

[40] Aarsh Shah, Tejas S Pandya, Damian Stoddard, Suman Babu Ukyam, Jason Street, James Wooten, Brian Mitchell; “Dynamic response of wood based bio-composites under high-strain rate compressive loading.” Journal of Wood and Fiber Science, 2017.

[41] “Natural frequency changes due to damage in composite beams”, I Negru, G R Gillich1, Z I Praisach1, M Tufoi, N Gillich. 11th International Conference on Damage Assessment of Structures (DAMAS 2015), IOP Publishing, Journal of Physics: Conference Series 628 (2015) 012091 doi:10.1088/1742-6596/628/1/012091

[42] Ján Svoreň, Ľubomír Javorek, Adam Droba, Dušan Paulíny; “Comparison of Natural Frequencies Values of Circular Saw Blade Determined by Different Methods”. doi:10.5552/drind.2015.1316.

[43] Jaime Horta-Rangel, Socorro Carmona, Victor M. Castaño, (2008) "Shift of natural frequencies in earthquake-damaged structures: an optimization approach", Structural Survey, Vol. 26 Issue: 5, pp.400-410, https://doi.org/10.1108/02630800810922748Carrera E 2004

[44] “Natural Frequency Shift in a Centrifugal Compressor Impeller for High-Density Gas Applications”; Yohei Magara, Haruo Miura, Naohiko Takahashi, Mitsuhiro Narita; DOI: 10.1115/1.4006423;http://turbomachinery.asmedigitalcollection.asme.org/pdfaccess.ashx?url=/data/journals/jotuei/926696

[45] Assessment of theories for free vibration analysis of homogeneous and multilayered plates Shock Vib. 11(3-4) 261-70

[46] Hause T and Librescu L 2006 Flexural free vibration of sandwich flat panels with laminated anisotropic face sheets J. Sound Vib. 297 823–41

[47] Gillich G R, Praisach Z I, Wahab M A and Vasile O 2014 Localization of transversal cracks in sandwich beams and evaluation of their severity Shock Vib. 9(4-5) 607125

[48] Moslemi AA. Dynamic viscoelasticity in hardboard. Forest Prod J 1967;17(1):25–33.

[49] Ross RJ, Pellerin RF. Nondestructive testing for assessing wood members in structures: a review. USDA Forest service Forest Products Laboratory, General tech. rep. FPL-GTR-70; 1994.

[50] Ilic J. Dynamic MOE of 55 species using small wood beams. Holz Roh Werkst, 2003;61(3):167–72.

[51] Measurement of dynamic modulus of elasticity and damping ratio of wood-based composites using the cantilever beam vibration technique. Zheng Wanga,, Ling Li, Meng

Gong. Journal of Construction and building materials. doi:10.1016/j.conbuildmat.2011.09.001

[52] Finite Element Analysis of Wheel Rim Using Abaqus Software Bimal Bastin, Adars S, Akshay Madhu, Arun Krishnan, Betson Jose, Praveen Raj. Int. Journal of Engineering Research and Application ;ISSN : 2248-9622, Vol. 7, Issue 2, (Part -1) February 2017, pp.31-34

[53] Non-circular gear modal analysis based on ABAQUS; Zhou Kaihong, Li Yunpeng, Wang Congyi,Li Cheng. 2015 8th International Conference on Intelligent Computation Technology and Automation

[54] Nilesh K.Kharate, Dr. Sharad S.Chaudhari; "Investigation of Natural Frequency and Modal Analysis of Brake Rotor Using Fea and Ema"; International Journal of Innovative Research in Science, Engineering and Technology; Vol. 3, Issue 10, October 2014. DOI: 10.15680/IJIRSET.2014.0310013

[55] Determination of orthotropic bone elastic constants using FEA and modal analysis. W.R. Taylora, E. Rolandb, H. Ploegc, D. Hertigc, R. Klabundec, M.D. Warnera, M.C. Hobathod, Rakotomananab, S.E. Clifta, Journal of Biomechanics 35 (2002) 767–773

[56] Standard Test Method for Poisson's Ratio at Room Temperature. ASTM Designation: E 132 – 04.

[57] Date palm fibers and natural composites. In: Postgraduate symposium on composites science and technology 2014 & 4th postgraduate seminar on natural fibre composites 2014, 28/01/2014, Putrajaya, Selangor, Malaysia

[58] AL-Oqla FM, Sapuan SM (2014b) Enhancement selecting proper natural fiber composites for industrial applications. In: Postgraduate symposium on composites science

and technology 2014 & 4th postgraduate seminar on natural fibre composites 2014, 28/01/2014, Putrajaya, Selangor, Malaysia)

[59] Sapuan SM, Pua F-l, El-Shekeil Y, AL-Oqla FM (2013) Mechanical properties of soil buried kenaf fibre reinforced thermoplastic polyurethane composites. Mater Des 50:467–470

[60] Love, A. E. H. A Treatise on the Mathematical Theory of Elasticity (Dover, 1944)

[61] Poisson's ratios of an oriented strand board; W.H. Thomas; Wood Sci Technol 37 (2003) 259–268 DOI 10.1007/s00226-003-0171-y

[62] Determination of Poisson's ratios in relation to fiber angle of a tropical wood species Nilson Tadeu Mascia , Elias Antonio Nicolas http://dx.doi.org/10.1016/j.conbuildmat.2012.12.014

[63] Poisson's ratio values for rocks doi:10.1016/j.ijrmms.2006.04.011 H. Gercek

[64] (Influence of a wide range of moisture contents on the Poisson's ratio of wood; Mayu Mizutani, Kosei Ando J Wood Sci (2015) 61:81–85 DOI 10.1007/s10086-014-1438-7)

[65] Designation: E 132 – 04 Standard Test Method for Poisson's Ratio at Room Temperature1

[66] Khaled T. S. Hassan, Petr Horáček, Jan Tippner, Evaluation of Stiffness and Strength of Scots Pine Wood Using Resonance Frequency and Ultrasonic Techniques, 2013 DOI: 10.15376/biores.8.2.1634-1645

VITA

AARSH J SHAH

aarsh.fb@gmail.com | (847) 797 4626 www.linkedin.com/in/aarsh-shah

EDUCATION

- M. S. in Mechanical Engineering

  The University of Mississippi~OleMiss, MS, USA

  Graduated 9th December 2017

- B. S. in Mechanical Engineering

  Dharamsinh Desai University, India

  Graduated on 9th May 2015

TEACHING EXPERIENCE

- **The University of Mississippi,** ***Teaching Assistant***

  ME324- Introduction to Mechanical Design (Spring 2016, Spring 2017),

  ME325- Intermediate Dynamics (Fall 2016)

  ME406- Alternative Energy Systems (Fall 2016),

  ME541- Theory and Use of CAD and Solid Modeling, CREO (Fall 2016, Winter 2017, Fall 2017). Assisted over 100 BSME students.

RESEARCH

- **The University of Mississippi**

  Worked on Split Hopkinson Pressure Bar, MTS Machines, Shock Tube and other equipment to test High Strain rate behavior of bio-composites, vibrational characteristics. Worked on developing different testing methods as per requirements.